TRANSCRIPTIONAL REGULATION OF MUSCLE CONTRACTILITY AND METABOLISM BY A MICRORNA-MEDIATED FEED FORWARD LOOP

APPROVED BY SUPERVISORY COMMITTEE

Eric N. Olson, Ph.D

_____

James Stull, Ph.D

_____

Steven A. Kliewer, Ph.D

_____

Joseph A. Hill, M.D., Ph.D

_____

Dedicated to my wife Elizabeth and to my parents

TRANSCRIPTIONAL REGULATION OF MUSCLE CONTRACTILITY AND METABOLISM BY A MICRORNA-MEDIATED FEED FORWARD LOOP

by

DANIEL S. QUIAT

DISSERTATION

Presented to the Faculty of the Graduate School of Biomedical Sciences

The University of Texas Southwestern Medical Center at Dallas

In Partial Fulfillment of the Requirements

For the Degree of

DOCTOR OF PHILOSOPHY

The University of Texas Southwestern Medical Center at Dallas

Dallas, Texas

February, 2012

TRANSCRIPTIONAL REGULATION OF MUSCLE CONTRACTILITY AND METABOLISM BY A MICRORNA-MEDIATED FEED FORWARD LOOP

DANIEL S. QUIAT, Ph.D

The University of Texas Southwestern Medical Center at Dallas, 2012

Supervising Professor: **ERIC N. OLSON Ph.D.**

In response to physiological stimuli, skeletal muscle alters its myofiber composition to significantly affect muscle performance and metabolism. This process requires concerted regulation of myofiber specific isoforms of sarcomeric and calcium regulatory proteins that couple action potentials to the generation of contractile force, and a concordant alteration of myofiber metabolism. This stress responsive phenotypic shift requires that extrinsic and intrinsic signals coordinately affect gene regulatory mechanisms to ensure a proper adaptive response.

Messenger RNA transcripts coding for three myosin heavy chain contractile proteins, *Myh6, Myh7, and Myh7b*, encode microRNAs miR-208a, miR-208b, and miR-499 respectively, within their introns. Here, I demonstrate through gain and loss of function studies *in vivo* that this family of microRNAs, termed MyomiRs, functions in skeletal muscle to promote the conversion of glycolytic myofibers expressing fast isoforms of contractile proteins, to slow oxidative myofibers that confer improved muscular performance. The MyomiRs influence myofiber phenotype by negatively regulating the transcription factor Sox6, in addition to several other functionally related transcriptional repressors.

Subsequent studies identified Sox6 as a fast myofiber enriched repressor of slow muscle gene expression. Mice lacking Sox6 specifically in skeletal muscle have an increased number of slow myofibers, elevated mitochondrial activity, and exhibit down regulation of the fast myofiber gene program, resulting in enhanced muscular endurance. This effect on skeletal muscle is mediated by the direct binding of Sox6 to conserved cis-regulatory elements upstream of slow myofiber enriched genes, leading to their transcriptional repression.

Collectively, these results identify myosin heavy chain encoded microRNAs, and their target Sox6, as robust regulators of muscle contractile and metabolic phenotype, and elucidate a double negative feed-forward regulatory loop by which functionally related fiber type specific gene isoforms are collectively controlled in response to physiological stressors.

TABLE OF CONTENTS

PRIOR PUBLICATIONS

Quiat D., Voelker K.A., Pei J., Grishin N.V., Grange R.W., Bassel-Duby R., Olson E.N. (2011). Concerted regulation of myofiber-specific gene expression and muscle performance by the transcriptional repressor Sox6. Proc Natl Acad Sci U S A. Jun 21;108(25):10196-201.

van Rooij, E., **Quiat, D.**, Johnson, B.A., Sutherland, L.B., Qi, X., Richardson, J.A., Kelm, R.J., Jr., and Olson, E.N. (2009). A family of microRNAs encoded by myosin genes governs myosin expression and muscle performance. Dev Cell 17, 662-673.

LIST OF FIGURES

LIST OF TABLES

LIST OF ABBREVIATIONS

miR - microRNA

SRF – serum response factor

MEF2 – myocyte enhancer factor 2

MyoD – myogenic differentiation 1

SOL - soleus

TA – tibealis anterior

EDL – externsor digitorum longus

ATP – adenosine triphosphate

Myh – myosin heavy chain

NFAT – nuclear factor of activated T-cells

PGC - Peroxisome proliferator-activated receptor gamma coactivator

PPAR - peroxisome proliferator-activated receptor

SOX - *Sry*-related HMG box containing transcription factor

MCIP1- Myocyte enriched calcineurin interacting protein 1

CHAPTER I

SKELETAL MUSCLE FIBER DIVERSITY: ORIGINS AND FUNCTION

Introduction

The use of active locomotion as a means to seek out nutrients and avoid noxious stimuli is essential for the survival of many organisms. Simple prokaryotes and eukaryotes, with their minimal size and often-aqueous environment, utilize molecular motors, such as cilia and flagella, for movement. In contrast, animals have complex body plans and are relatively larger in size, and have evolved specialized skeletal and muscular organ systems for support and motion. The rudimentary skeletal muscle of simple animals (Martindale, 2005; Seipel and Schmid, 2005) has further diversified to accommodate for different contractile and metabolic needs of various muscle groups, and to function as a key regulator of glucose homeostasis and metabolism (Parrizas et al., 1995).

In 1873, French Scientist Louis Ranvier first documented heterogeneity in skeletal muscle fiber types, identifying red 'slow' and while 'fast' myofibers in dissected rabbit skeletal muscle (Ranvier, 1873). Approximately one and a half centuries since this seminal observation, muscle fiber types with differing

metabolic and contractile properties have been identified in a range of organisms, from invertebrates (Wiersma, 1952) to humans, and much work has focused on characterizing their molecular properties, physiological function, and developmental regulation. Information garnered from these studies has profoundly affected the fields of human exercise physiology, cardiology, and metabolism, and has identified potential avenues for therapeutic treatment of musculoskeletal disease and type II diabetes.

Biochemical and molecular properties

The sarcomere

The striated appearance of skeletal muscle arises from the tandem arrangement of individual contractile units termed sarcomeres. Each sarcomere is composed of thick filaments intercalated between Z-disk-bound thin filaments (Figure 1.1). Sarcomeric contraction occurs when thick filament myosins bind to actin thin filaments, and hydrolyze ATP to generate a power stroke (Spudich, 2001). This process is tightly regulated by the calcium sensitive troponin-tropomyosin complex, which alters its conformation to permit actin-myosin interactions in response to increased intracellular calcium following motor-neuron induced depolarization (Bruce Alberts, 2002; Lehman et al., 1994). Multiple isoforms of contractile apparatus proteins are regulated in a fiber-type specific manner, and can profoundly influence overall muscle function (Bandman, 1992).

For example, differential expression of myosin heavy chain (Myh) isoforms alters force-velocity parameters of individual muscle fibers, while alternate combinations of troponin T, I and C isoforms influence myofiber Ca^{2+} sensitivity (Bottinelli et al., 1991; Geiger et al., 1999). The mechanism by which contractile and calcium regulatory genes are concordantly regulated to produce a unified effect on muscle contraction is poorly understood.

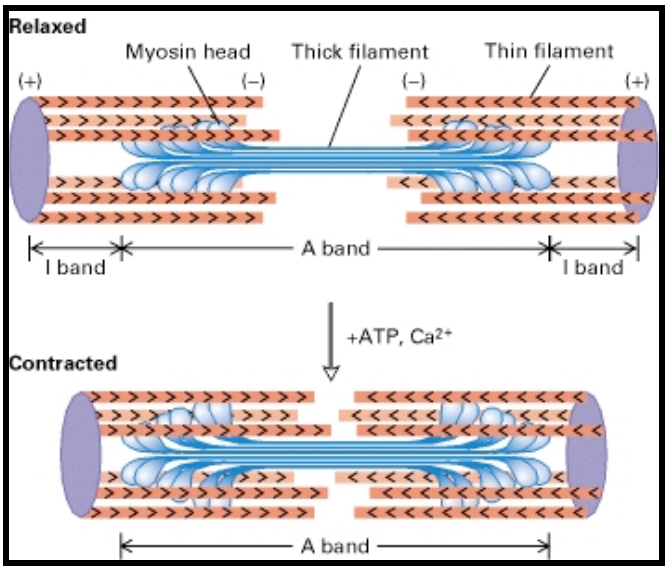

Figure 1.1. Schematic representation of sarcomere contraction in response to increased intracellular calcium (Harvey Lodish, 2000).

Muscle fiber types

Skeletal muscle is composed of a heterogeneous population of slow and fast myofibers that display contrasting contractile and metabolic properties. Slow type I fibers exhibit oxidative metabolism, express slow isoforms of sarcomeric

proteins, and are classically identified by their expression of type I myosin heavy chain (Myh7 or β-myosin heavy chain). In contrast, fast type IIa, IIx/d, and IIb myofibers utilize glycolytic metabolism, express fast isoforms of contractile proteins, and are designated by their expression of fast myosin heavy chain isoforms; Myh2, Myh1, and Myh4, respectively (Bassel-Duby and Olson, 2006). While these characteristics are classically used to define muscle fibers in concrete terms, in reality, myofibers are hybrids that variably express myosin heavy chain and other sarcomeric protein isoforms along their length (Staron et al., 1987). Additionally, muscle fiber type content of a specific muscle group is plastic and can be altered in response to physical or metabolic stress.

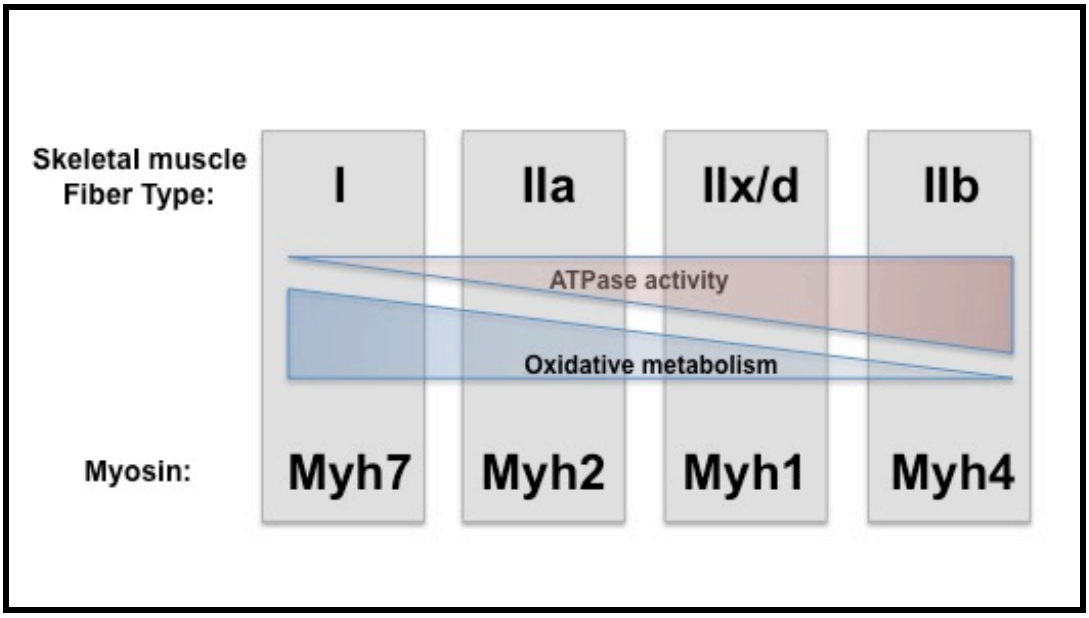

Figure 1.2. Relationship between muscle fiber type, myosin heavy chain isoform gene expression, and metabolism.

Muscle fiber type contractile properties

It has long been recognized that slow type I and fast type II muscle fibers display unique contractile properties. Measurements of muscle performance under electrical stimulation *ex vivo* and *in vivo* have been used to elucidate these differences (Brooks and Faulkner, 1988; Brooks et al., 1990). Slow skeletal muscle, rich in type I fibers, generates less contractile force and demonstrates a slower velocity of contraction compared to fast myofiber enriched muscle. Type I myofibers are also able to maintain an higher percentage of their maximal force during constant stimulation, while fast muscle groups fatigue, and loose the ability to generate force more rapidly. Last, type I myofibers exhibit improved recovery after stimulation, and are able to generate a higher percentage of their maximal force following fatigue when compared to fast type II myofibers. Cumulatively, these studies demonstrate that regulation of skeletal muscle fiber type profoundly affects muscle performance.

Transcriptional regulation of myofiber identity

Calcium induced signaling

Chronic muscle stimulation induces a reversible transition in myofiber phenotype from fast to slow, which occurs in a sequential manner through several fast myofiber intermediates (type IIb ➔ type IIx/d ➔ type IIa ➔ type I) (Pette and Staron, 2000). Therefore, physical conditions that lead to alterations in the

frequency of muscle stimulation affect muscle fiber type. Endurance exercise results in the conversion of fast myofibers towards a slow, fatigue resistant phenotype, while decreased muscle usage results in a loss of slow myofibers (Allen et al., 2001; Templeton et al., 1988). Persistent muscle stimulation results in increased calcium transients, which activate the calcium-sensitive signaling serine/threonine phosphatase calcineurin. In turn, calcineurin dephosphorylates the transcription factor NFAT to induce its cytoplasmic to nuclear shuttling, allowing NFAT to transactivate target genes in the nucleus (Crabtree and Olson, 2002). Transgenic over-expression of activated calcineurin in skeletal muscle was sufficient to induce conversion of myofibers from fast to slow, recapitulating the phenotype that occurs following an increase in calcium transients (Naya et al., 2000). Conversely, inhibition of calcineurin by transgenic over-expression of the inhibitory molecule MCIP1 or pharmacological treatment with the calcineurin antagonist cyclosporine A, prevents conversion of stimulated skeletal muscle fibers from fast to slow (Chin et al., 1998; Wu et al., 2001).

Mef2

Myocyte enhancer factor 2 (Mef2) is a member of the MADS family of transcription factors that is enriched in cardiac and skeletal muscle, and mediates stress responsive gene expression (Potthoff and Olson, 2007). Under normal physiological conditions, Mef2 activity in skeletal muscle is repressed by histone

deacetylaces (HDACs) (McKinsey et al., 2001). Stress induced activation of multiple signaling cascades results in HDAC sequestration in the cytoplasm and permits Mef2 transcriptional activity. Exercise training in mice induced calcium-dependent activation of Mef2 activity (Wu et al., 2001). Genetic deletion of Mef2 *in vivo* demonstrated that Mef2 was partially required for slow myofiber formation, while transgenic over-expression of a Mef2-VP16 fusion protein specifically in skeletal muscle was sufficient to drive fast to slow myofiber conversion (Potthoff et al., 2007). Multiple studies have demonstrated that Mef2 and calcium-induced NFAT activity synergize to directly active the transcription of genes enriched in slow myofibers (Calvo et al., 1999; Chin et al., 1998; Crabtree and Olson, 2002).

Thyroid hormone

Thyroid hormone is a powerful regulator of embryonic development and metabolic homeostasis. Gene expression governing cardiac and skeletal muscle contractility is strongly influenced by thyroid hormone levels. The hyperthyroid state is associated with cardiac tachyarrhythmias and an increase in fast myofibers in skeletal muscle, while the hypothyroid state is associated with cardiac bradycardia and slow contractile gene expression in skeletal muscle (Baldwin and Haddad, 2001). Pharmacological treatment with thyroid hormone agonists strongly elicited a switch from slow to fast myosin expression in skeletal muscle

(Larsson et al., 1995), while thyroid hormone antagonism or genetic deletion of the thyroid hormone receptor increased the proportion of slow skeletal muscle fibers (McAllister et al., 1991; Yu et al., 2000). This effect is mediated, in part, by the direct action of thyroid hormone receptor on an enhancer upstream of the *Myh7* locus (Wright et al., 1999).

Metabolic regulators of fiber type

Contractile protein isoform expression in a myofiber type strongly correlates with metabolic properties, suggesting that these two characteristics might be under the control of common regulatory elements. The peroxisome proliferator-activated receptor (PPAR) family of nuclear hormone receptors binds to fatty acid derived ligands and regulates metabolic gene expression (Shulman and Mangelsdorf, 2005). PPARs and their related transcriptional co-activators, PGC-1α and PGC-1β, exhibit powerful and distinct roles in myofiber type specification.

Genetic gain and loss of function experiments demonstrated that PPARδ was necessary and sufficient to drive slow myofiber gene expression (Narkar et al., 2008; Schuler et al., 2006). Similarly, pharmacological activation of PPARδ increased oxidative metabolism and slow myofiber content in skeletal muscle, mimicking the effects of exercise training (Narkar et al., 2008). Recent work demonstrated that the influence of PPARδ on skeletal muscle fiber type was due,

at least in part, to a physical interaction with Mef2 that mediated slow myofiber specific gene expression (Gan et al., 2011).

PGC-1α is a transcriptional co-activator of nuclear hormone receptors that drives mitochondrial biogenesis and respiration in muscle (Wu et al., 1999). Transgenic over-expression of PGC-1α was sufficient to drive the formation of type I myofibers in mice via a Mef2 mediated mechanism (Lin et al., 2002). The closely related PGC-1β was sufficient to promote the formation of type IIx/d intermediate myofibers by directly regulating the expression of *Myh1* and promoting oxidative metabolism (Arany et al., 2007). Interestingly, genetic loss of both PGC-1 co-activators, either individually or in combination, did not effect the formation of slow myofibers *in vivo*(Zechner et al.).

Transcriptional regulation of fast myofiber genes

While the aforementioned regulatory pathways center on the transcriptional regulation of the slow myofiber gene program, very little is known about pathways that regulate fast myofiber formation. To date, the only factors identified to directly promote the formation of fast myofibers *in vivo* are Eya1 and Six1, which induce a switch towards fast myosin isoform expression and glycolytic metabolism (Grifone et al., 2004). This effect is mediated by direct binding of these factors to enhancer elements upstream of fast myofiber enriched genes, and cooperative activation with the transcription factor Mef3.

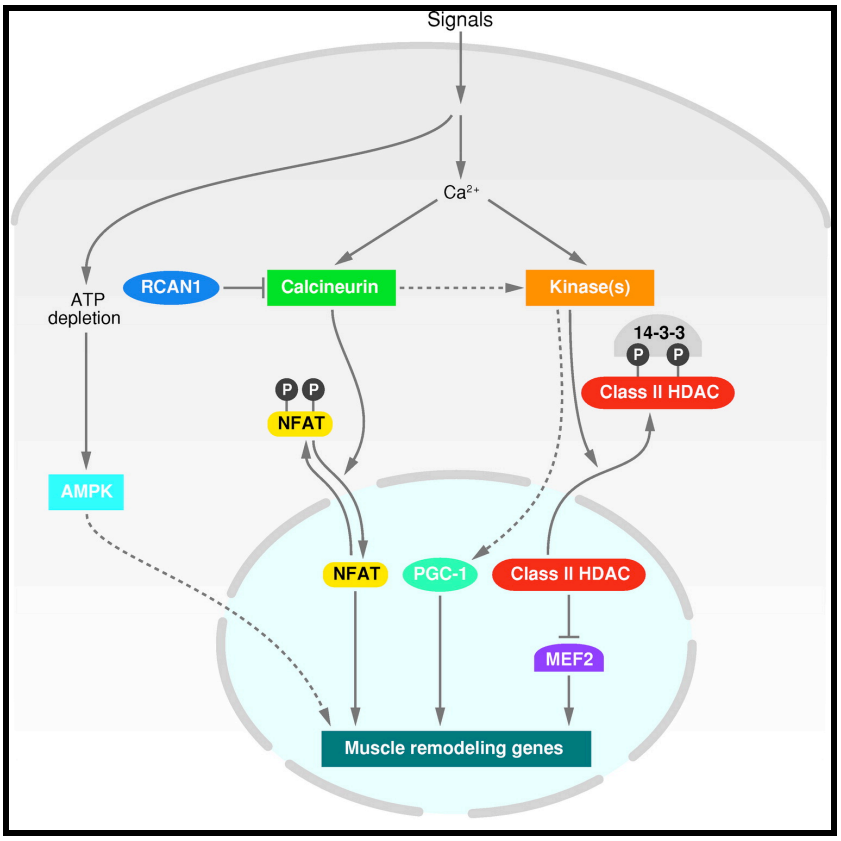

Figure 1.3. Transcriptional regulation of skeletal muscle remodeling

Muscle fiber types and disease

Neurological Disease

The muscle fiber type composition of skeletal muscle is frequently altered in the setting of musculoskeletal and neurological disease. In healthy skeletal muscle, myofibers of a similar type commonly share motor neuron input, designating them as a 'motor unit', and are stochastically interspersed with other fiber types (Buchthal and Schmalbruch, 1980). This random arrangement of

myofiber types is disrupted during many muscle pathologies, and results from motor unit denervation, followed by innervation from collateral motor neurons. Histologically, this leads to fiber type grouping, with myofibers of a given type arranged in ordered clusters (Karpati and Engel, 1968).

Loss of muscular innervation occurs in a variety of neurological pathologies and affects type I myofiber distribution. Spinal cord injury reduces motor neuron input to muscle groups and results in general muscular atrophy. This reduction in muscle mass is accompanied by a marked reduction in the proportion of type I myofibers (Figure 1.4), and by a decrease in markers of

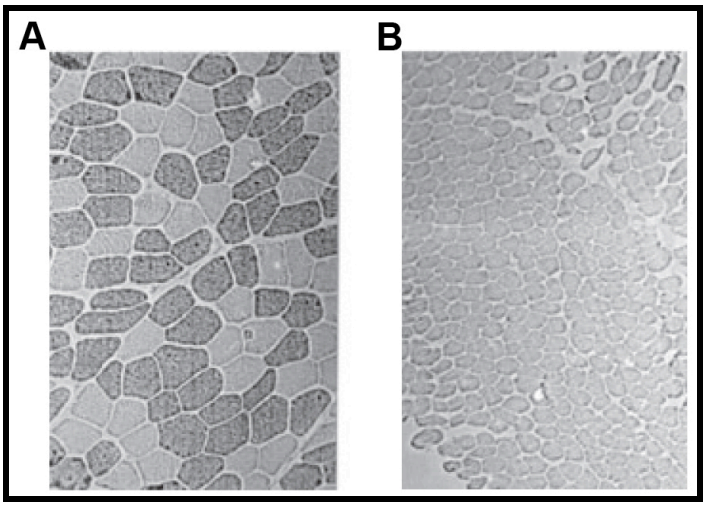

Figure 1.4. Loss of type I myofibers following paralysis
Staining for slow myosin in skeletal muscle biopsies from a spinal cord injury patient (B) and control (A) demonstrates a reduction in type I fibers and marked myofiber atrophy. Adapted from: (Schiaffino, 2011)

oxidative metabolism (Biering-Sorensen et al., 2009). In addition to the disappearance of type I myofibers, patients with spinal cord injury demonstrate an increase in the proportion of hybrid muscle fibers that express both slow and fast sarcomeric protein isoforms.

Conversely, several conditions are marked by an increase in type I myofiber content. Centronuclear myopathy and type I fiber predominance are clinically characterized by generalized muscle weakness, and muscle biopsy specimens from these patients demonstrate almost 100% type I myofiber content (Linssen et al., 1991). In addition, specific congenital mutations in the ryanodine receptor, a mediator of sarcoplasmic calcium release, lead to a complete conversion of skeletal muscle to type I myofibers (Sato et al., 2008).

Finally, fast and slow muscle fibers differ in their susceptibility to injury and repair. Atrophic conditions, such as spinal cord trauma, disuse, aging, and cachexia lead to a disproportionate reduction in the size of type II fast myofibers (Fiori et al., 1983; Lexell, 1995). Conversely, resistance training of muscle results in hypertrophy of type II myofibers, with little change in the size of type I myofibers (McCall et al., 1996). Transgenic mice that have a higher proportion of type I myofibers exhibited resistance to denervation induced atrophy, suggesting that modulation of skeletal muscle fiber type might be a therapeutic avenue for the preservation of muscle function during atrophic conditions (Sandri et al., 2006).

Metabolic disease

Skeletal muscle is a major metabolic organ that plays a key role in glucose homeostasis. Muscle fiber types differ in their ability to take up glucose from the blood, due to different rates of GLUT4 glucose transporter translocation to the plasma membrane in response to insulin signaling (Halseth et al., 2001)**.** This difference in insulin sensitivity between myofiber types suggests that myofiber composition of skeletal muscle could profoundly influence whole body glucose homeostasis.

Type II diabetes is characterized by a dysregulation of blood glucose levels due to progressive insulin resistance, and often presents in obese, inactive patients. A correlation between myofiber type content in skeletal muscle, and diabetes and obesity has been firmly established (Lillioja et al., 1987). Skeletal muscle of patients with a higher body mass index(BMI) and type 2 diabetes contained more fast type IIb myofibers (Tanner et al., 2002). As these patients lost weight and improved overall metabolic parameters, they showed an increase in type I myofibers.

Similar observations have been made in mouse models of diet-induced obesity. Genetic mouse models that have more type I muscle fibers in skeletal muscle, such the PPARδ and PGC-1α skeletal muscle specific transgenic mice, gained less weight and demonstrated improved glucose tolerance when placed on a high fat diet (Choi et al., 2008; Wang et al., 2004). Interestingly, a mouse model

that with increased mass of type II fibers due to activated AKT signaling also showed resistance to high fat diet induced obesity (Izumiya et al., 2008). Together, these studies suggest that genetic manipulations that increase type I oxidative fibers or glycolytic fiber mass in skeletal muscle can reduce the metabolic derangement that results from a high fat diet.

Concluding remarks

Since the initial observation of gross differences in skeletal muscle phenotype, much insight has been gained into the regulation and functional significance of myofiber diversity. Transcription factors associated with developmental gene programs or with the regulation of metabolism have been shown to influence the contractile and metabolic properties of a muscle fiber.

Several aspects of muscle fiber type biology are poorly understood. First, very little is known about the factors that regulate fast myofiber formation. One of the questions that remains is if activation of fast myofiber genes is achieved through direct transcriptional activation, or if it occurs in response to repression of the slow myofiber program, or a combination of both mechanisms. Additionally, it is unclear if the myofiber type transitions that are induced in the gain and loss of function studies mentioned here are identical. Perhaps the metabolic regulators primarily induce a metabolic shift that drives compensatory responses in sarcomeric gene expression, while the developmental and calcium sensitive

factors drive slow sarcomeric gene expression, accompanied by an indirect shift in metabolism. It seems likely that there are many points in which the contractile and metabolic gene programs influence each other via direct or indirect mechanisms. Investigation of muscle fiber type transitions in a simplified *in vitro* system could highlight the differences in the myofiber gene program induced by each genetic manipulation.

The numerous associations of muscle fiber type regulation in diseased patients are also of great interest. The correlation of myofiber type with obesity and glucose tolerance in type 2 diabetes is intriguing, however the causal role of this relationship needs to be scrutinized. Studies of mice containing predominantly type I myofibers suggest a causal role for muscle fiber type in glucose homeostasis in the setting of obesity. Further investigation of acute increases in type I myofiber content in the setting of diabetes, through use of inducible transgenic mice would be useful for understanding the muscle fiber type – obesity connection. These studies would highlight the potential use of pharmacological agents to therapeutically alter muscle fiber type for the recovery of muscle function in musculoskeletal disease, and to promote metabolic homeostasis in the setting of type II diabetes.

CHAPTER II

MICRORNAS IN MUSCLE DEVELOPMENT AND DISEASE

Introduction

The era of modern genomics has brought to light the interesting observation that neither genome size, nor gene number correlate with the overall complexity of an organism (Claverie, 2001). The current prevailing theory for the derivation of organismal complexity from relatively similar numbers of protein coding genes is that additional gene regulatory mechanisms exist in higher organisms, allowing for intricate phenotypes (Fickett and Wasserman, 2000; Struhl, 1999). Regulation of gene expression through non-conding RNAs (ncRNAs) is one such method that is hypothesized to contribute to eukaryotic complexity (Mercer et al., 2009).

MicroRNAs (miRNAs), small regulatory RNAs, were first identified through forward genetics in *C. elegans* as regulators of developmental timing (Moss et al., 1997; Reinhart et al., 2000). Further studies have identified miRNAs and other recently identified classes of ncRNAs as powerful regulators of gene expression during development and disease (Pauli et al., 2011; Salmena et al., 2011). While these studies have firmly established the importance of miRNA

function, much is still unknown about the mechanisms of miRNA action and their roles in complex gene regulatory networks.

MicroRNA biogenesis and function

MicroRNAs (miRs) are highly conserved RNAs, 18-25 nucleotides in length, that regulate gene expression. MicroRNAs are encoded within the genome as intronic miRs, which are located in and processed from introns of protein-coding gene transcripts, or as intergenic miRs that are transcribed under the control of their own promoters. Processing of the primary miR-encoding transcript (pri-miR) in the nucleus by Drosha produces a pre-miR stem loop 80-110 nucleotides in length. Exportin 5 facilitates nuclear export of the pre-miR to the cytoplasm, where it is then processed into a mature miRNA:miRNA* duplex by Dicer (Bartel, 2004). The mature miRNA is then loaded into the RNA-induced silencing complex (RISC) which targets the 3'-untranslated region (UTR) of transcripts to regulate expression. In the current paradigm of microRNA function, imperfect binding of a miR to its target mRNA prevents translation, while precise complementary binding results in target transcript degradation. Recent data suggests that the miRs primarily affect gene expression via subtle changes in mRNA transcript stability (Guo et al., 2010), thus resulting in small changes in protein levels (Baek et al., 2008). While the effects of any individual miR on a single target might be subtle, the combinatorial effects of a miR on multiple

mRNA targets within a regulatory network can profoundly change the output of a pathway.

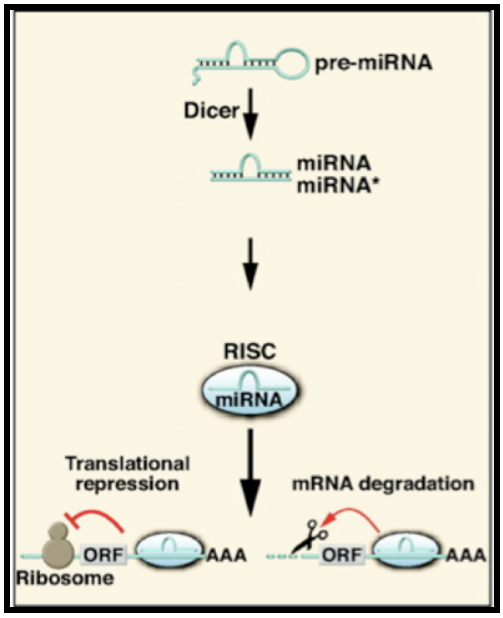

Figure 2.1. MicroRNAs are processed by Dicer and are incorporated into the RISC complex to induce gene silencing (van Rooij et al., 2008)**.**

MicroRNAs in skeletal muscle

Several evolutionarily conserved microRNAs display restricted expression in cardiac and skeletal muscle. The most abundant of these muscle specific miRs belong to the miR-1/206 and miR-133 microRNA families. MiR-1-1 and miR-1-2 are identical in sequence and are clustered at separate loci with miR-133a-2 and miR-133a-1 respectively. Both species of miR-133a share a homologous

sequence. Expression of miR-1-1/133a-2 and miR-1-2/133a-1 primary transcripts in cardiac and skeletal muscle is governed by the myogenic transcription factors MyoD, Mef2, and SRF (Liu et al., 2007). MiR-206 differs from miR-1 by 4 nucleotides and is clustered with miR-133b, which differs by 2 nucleotides from miR-133a. Transcription of the skeletal muscle specific miR-206/133b pri-miR is regulated by MyoD, which binds to cis-regulatory elements upstream of the miR-206 locus (Rao et al., 2006). *In vitro* studies in C2C12 myoblasts identified a role for miR-1 in promoting muscle differentiation via repression of its target HDAC4, and elucidated a function for miR-133 in myoblast proliferation by down-regulation of SRF (Chen et al., 2006). Similarly, over-expression of miR-206 was shown to promote the differentiation of C2C12 myoblasts *in vitro* (Kim et al., 2006).

An essential role for microRNAs in skeletal muscle *in vivo* was demonstrated when the RNase-III enzyme Dicer was conditionally ablated from embryonic skeletal muscle, resulting in perinatal lethality (O'Rourke et al., 2007). Embryonic skeletal muscle from these mice was hypoplastic and a demonstrated a significant increase in apoptosis, suggesting that Dicer-mediated processing of microRNAs was required for normal muscle development.

Several studies have utilized genetic loss of function of elucidate the role of individual muscle specific miRs *in vivo*. A subset of mice carrying null alleles for miR-133a1/133a2 exhibited lethality due to defects in cardiac development

(Liu et al., 2008). MiR-133a1/133a2 knockout mice that survived to adulthood suffered from progressive centronuclear myopathy, which resulted from the over-expression of the miR-133a target gene dynamin-2 (Liu et al., 2011). Mice lacking miR-206 appeared phenotypically normal; however, these mice displayed dysfunctional neuromuscular junction reinnervation in response to surgical or disease-associated denervation (Williams et al., 2009).

Concluding remarks

These studies underscore the general importance of microRNA regulatory networks in muscle and the roles of individual microRNAs in specific muscle pathologies. The functions of several other microRNAs that display muscle specificity, such as miR-1 and miR-133b, remain to be characterized *in vivo*. Additionally, other microRNAs with broad expression patterns, such as let-7, miR-26, and miR-101, are among the most abundantly expressed microRNAs in skeletal muscle (Nielsen et al., 2010). Genetic studies of these miRs *in vivo* will further elucidate the role of microRNAs in skeletal muscle biology. Finally, the therapeutic knockdown or over-expression of miRs in skeletal muscle remains to be studied as a means to treat myopathy and denervation atrophy that is associated with amyotrophic lateral sclerosis (ALS).

CHAPTER III

MYOSIN-ENCODED MICRORNAS GOVERN MYOFIBER PHENOTYPE

Abstract

Myosin is a key regulator of muscle strength and contractility. Here we show that three myosin genes, *Myh6*, *Myh7*, and *Myh7b*, encode related microRNAs within their introns, which, in turn, control muscle myosin content, myofiber identity and muscle performance. In skeletal muscle, two slow myosins and their intronic miRNAs, Myh7/miR-208b and Myh7b/miR-499, respectively, are co-expressed. MiR-208b and miR-499 are functionally redundant, and play a dominant role in the specification of muscle fiber identity by activating slow and repressing fast myofiber gene programs. The actions of these miRNAs are mediated by a collection of transcriptional repressors of slow myofiber genes. These findings reveal that myosin genes not only encode the major contractile proteins of muscle, but also act more broadly to influence muscle function by encoding a network of intronic miRNAs that control muscle gene expression and performance.

Introduction

The heart and skeletal muscle are major contractile organs, whose performance is regulated by the expression of alternative isoforms of contractile myosin proteins with unique efficiencies of force generation. In the heart, this is exemplified by the switch from β-myosin heavy chain (β-MYH) to α-myosin heavy chain (α-MYH) in response to increased post-natal cardiac demand (Lompre et al., 1984), and the converse shift from α-MYH to β-MYH that is associated with reduced cardiac function during pathological stress remodeling (Nadal-Ginard and Mahdavi, 1989). In skeletal muscle, myofibers shift their expression of myosin from fast to slow isoforms in response to chronic electrical stimulation, endurance exercise, or hypothyroidism (Pette and Staron, 2000). The transcriptional mechanisms that control myosin switching are poorly understood and are key to understanding the mechanisms of decreased muscle performance in the diseased state.

Signature patterns of microRNA regulation have been observed following a variety of cardiac and skeletal muscle pathologies (Eisenberg et al., 2007; van Rooij et al., 2006). A recent study identified miR-208a, a cardiac enriched microRNA encoded within an intron of α-MYH (Myh6), as a regulator of the cardiac stress response. Remarkably, genetic loss of miR-208a in mice revealed that this microRNA was required for pathological remodeling during pressure-overload induced cardiac hypertrophy, and for a thyroid hormone dependant

switch in sarcomeric contractile machinery (van Rooij et al., 2007). Specifically, mice lacking miR-208a failed to up-regulate slow contractile genes in response to pharmacological blockade of thyroid hormone signaling. Subsequent bioinformatic analysis predicted the existence of miR-208b and miR-499, microRNAs encoded within the introns of two other myosin heavy chain isoforms, β-MYH (Myh7) and Myh7b respectively.

Using gain and loss of function genetics in mice, we identified that miR-208b/499 redundantly mediate a transcriptional regulatory network that reinforces slow myofiber gene expression in skeletal muscle via a reciprocal negative feedback loop (van Rooij et al., 2009). In this pathway, miRNAs miR-499 and miR-208b, intronically encoded within slow myosin heavy chain genes, target a collection of transcriptional repressors, and promote a fast to slow myofiber type switch.

Results

A family of miRNAs encoded by myosin genes

MiR-208a is encoded by intron 27 of the mouse *α-MHC* gene, which is expressed specifically in the heart (Fig. 3.1A and 3.1B). Because of the important role of miR-208a in regulating cardiac gene expression in response to stress (Callis et al., 2009; van Rooij et al., 2007), we scanned other myosin genes for possible intronic miRNAs. We discovered that intron 31 of the mouse *β-MHC*

gene is predicted to encode a closely related miRNA, miR-208b, which has an identical seed sequence to miR-208a and differs at only three nucleotides in the 3' region (Fig. 3.1A). miR-208b is co-expressed with *β-MHC*, showing highest expression in soleus muscle, which is comprised predominantly of slow type I myofibers, and lower expression in adult heart (Fig. 3.1B). A third member of this miRNA family, miR-499, is encoded by intron 19 of the mouse *Myh7b* gene (McGuigan et al., 2004), a little studied myosin gene that shares extensive homology with *β-MHC* (Fig. 3.1A). Myh7b and miR-499 are highly expressed in the heart and are enriched in the soleus, compared with gastrocnemius/plantaris (GP), tibialis anterior (TA), or extensor digitorum longus (EDL) muscles, which contain predominantly fast myofibers (Fig. 3.1B). We refer to this family of miRNAs as MyomiRs, because of their location within and co-expression with their corresponding myosin genes.

Generation of miR-499 and miR-208b null mice

To further explore the functions of miR-499 and miR-208b in vivo, we generated mutant mice with germ line deletions of the pre-miR regions of the *Myh7b* and *β-MHC* introns encoding these miRNAs, respectively. LoxP sites were introduced into the corresponding intron at both ends of the miR-208b-coding region (Fig. 3.2A). Breeding of these mice to mice expressing a CAG-Cre transgene, which is expressed ubiquitously, allowed for deletion of the

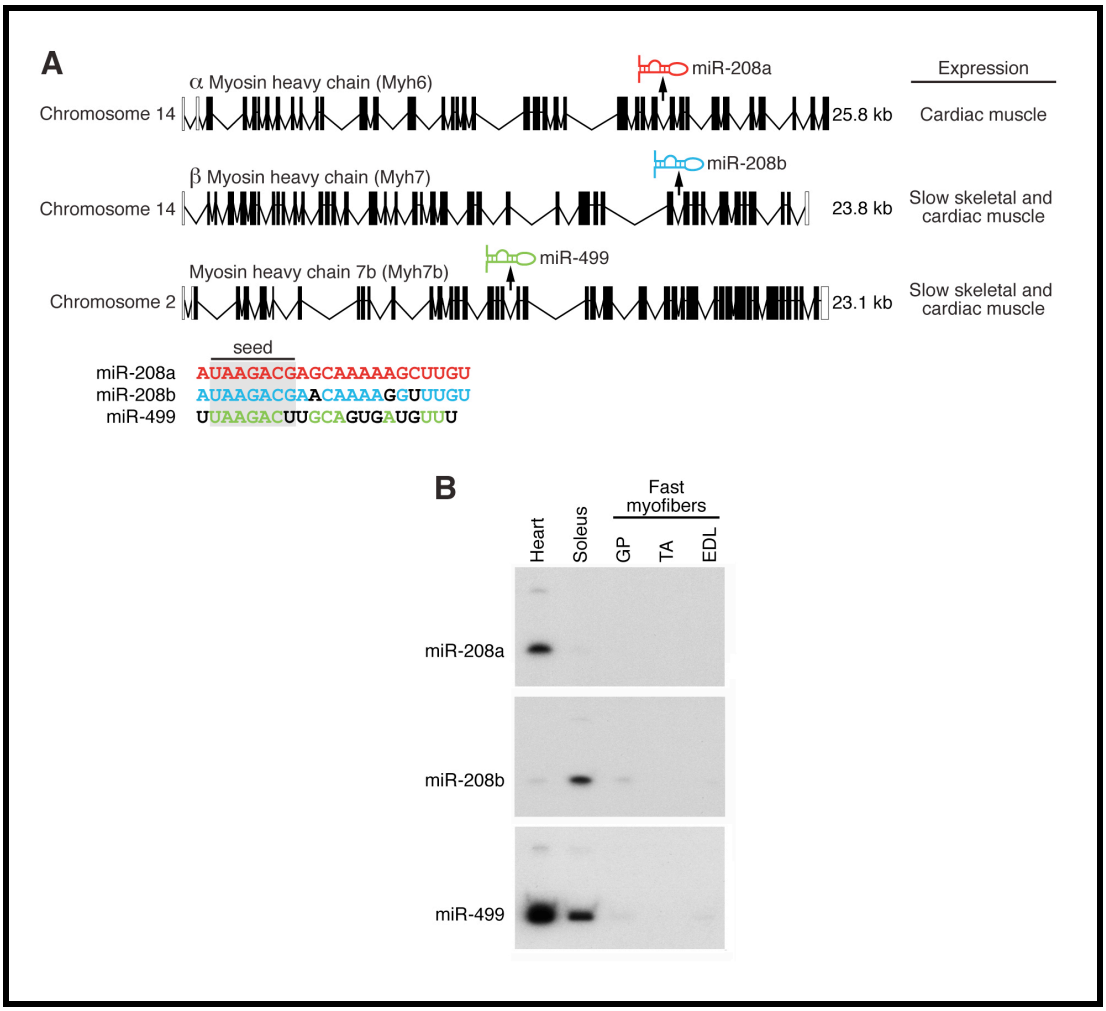

Figure 3.1. Distinct expression patterns of MyomiRs

(**A**) Schematic representation of the genomic location of the miRNAs present in the different myosin genes. miR-208a and -208b share a comparable seed region (nt 2-8) but differ at three bases in their 3' end (indicated in black). The seed region of miR-499 overlaps by 6 nt with miR-208 but differs significantly in the 3' region.

(**B**) Northern analysis shows that miR-208a expression correlates with the cardiac-specific expression of a-MHC, while miR-208b parallels the predominant slow skeletal expression of β-MHC. miR-499 is co-expressed with Myh7b, a slow myosin that is mainly expressed in the heart and soleus, a slow skeletal muscle, but not in fast myofibers. Label indicates the mature miRNA.

corresponding miRNA and its complete absence in homozygous mutant animals as shown by PCR using primers flanking the loxP site (Fig. 3.2B). miR-208b$^{-/-}$ mice were obtained at Mendelian ratios from heterozygous intercrosses and displayed no overt abnormalities (data not shown).

Mir-499$^{-/-}$ mice were generated previously in the lab. In these mice, Myh7b mRNA expression was unaltered in hearts, while there was a decrease in the soleus as detected by RT-PCR using primers in exons flanking the deletion in intron 19 (data not shown). Western blot analysis for both α-MHC and β-MHC, showed no difference between hearts from wild-type or miR-499$^{-/-}$ mice, and a comparable up-regulation in β-MHC expression in wild-type and miR-499$^{-/-}$ mice in response to PTU (data not shown).

Deletion of miR-208b did not alter *Myh7* transcript processing as determined by both RT-PCR using primers in exons flanking the deletion in intron 31 (Fig. 3.2C), or β-MHC expression by western blot analysis of neonatal cardiac tissue from miR-208b$^{-/-}$ mice (Fig. 3.2D). Thus in this MyomiR null mice, *β-MHC* and *Myh7b* host gene expression was not adversely effected, while the expression of their corresponding intronic miRNAs miR-499 and miR-208b was successfully ablated.

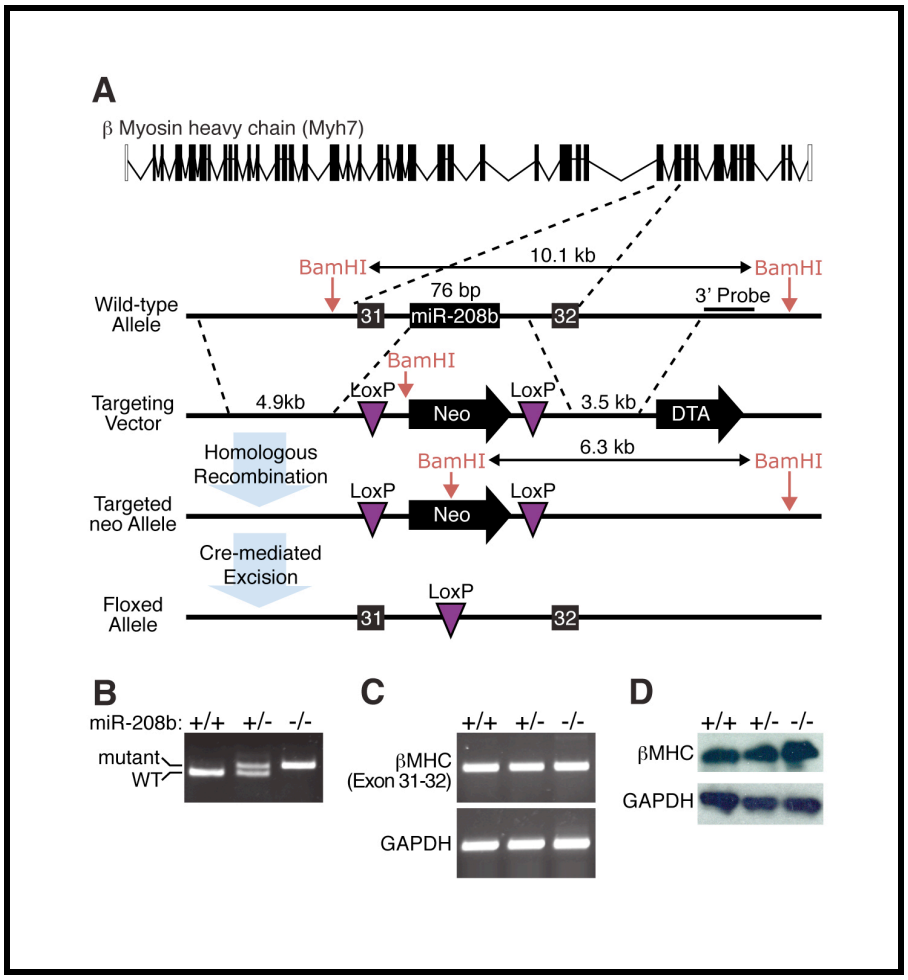

Figure 3.2. Generation of miR-208b null mice

(**A**) Strategy to generate miR-208b mutant mice by homologous recombination. The pre-miRNA sequence was replaced with a neomycin resistance cassette flanked by loxP sites. The neomycin cassette was removed in the mouse germline by breeding heterozygous mice to transgenic mice harboring the CAG-Cre transgene.

(**B**) Detection of the miR-208b mutation by PCR. Primers flanking the loxP site in intron 31 of the *b-MHC* gene generate PCR products as indicated.

(**C**) Detection of b-MHC expression by RT-PCR of RNA from hearts of mice of the indicated genotypes using primers flanking intron 31. Deletion of miR-208b does not disrupt expression of β -MHC.

(**D**) Detection of β-MHC by western blot analysis of heart from P0 mice of the indicated genotypes, showing that β-MHC expression is not altered by deletion of miR-208b. GAPDH was detected as a loading control.

Control of skeletal muscle fiber type by miR-499 and -208b

The cardiac specificity of miR-208a led us to investigate the potential involvement of miR-208b and miR-499 in the control of skeletal muscle fiber types. Deletion of either miR-208b or miR-499 did not alter the expression of the other miRNA in the soleus (data not shown), and fiber type analysis showed little or no difference in the number of type I myofibers in either of these mutant mice compared to wild-type (Figure 3.3A).

Wondering whether the homology of miR-208b and miR-499 and their coexpression in soleus might allow for redundant functions that were masked in mice with either single gene deletion, we generated miR-208b$^{-/-}$; miR-499$^{-/-}$ double knockout (dKO) mice. These mice were obtained at predicted Mendelian ratios from transheterozygous intercrosses and displayed no overt abnormalities. However, staining of histological sections for myofiber type with metachromatic ATPase stain and immunohistochemistry against β-MHC showed a substantial loss of type I myofibers in the soleus of dKO mice (Fig. 3.4A and 3.4B). The loss of slow myofibers in dKO mice was also evidenced

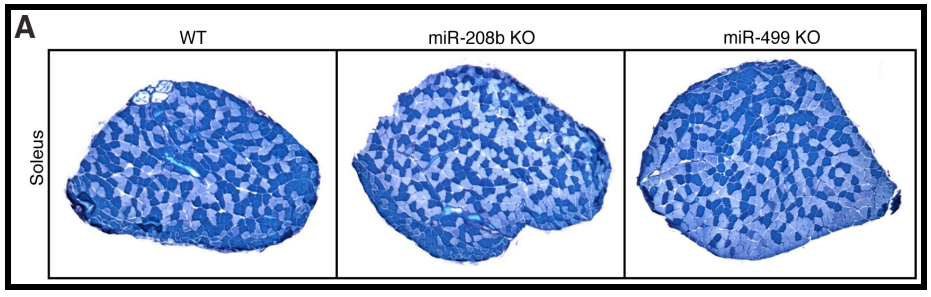

Figure 3.3 Normal fiber type distribution in miR-208b and miR-499 KO soleus muscle.

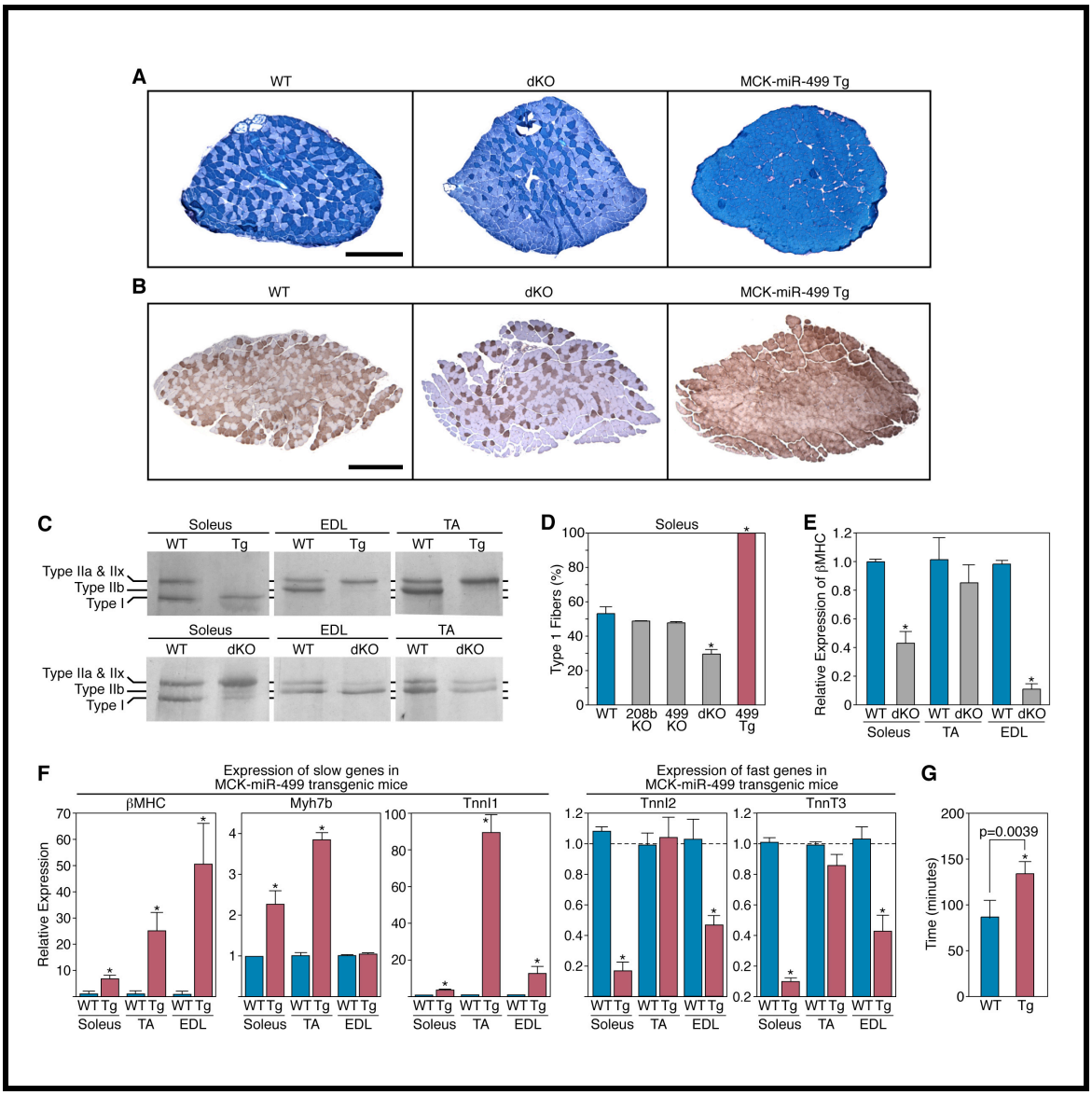

Figure 3.4. Control of skeletal muscle fiber type by miR-208b and miR-499
(**A**) Detection of type I myofibers in soleus of wild-type, miR-208b$^{-/-}$/miR-499$^{-/-}$ dKO, and MCK-miR-499 transgenic mice by metachromatic ATPase staining. Scale bar, 500 μm.
(**B**) Immunohistochemistry for βMHC to identify type I myofibers in the soleus of wild-type, miR-208b$^{-/-}$/miR-499$^{-/-}$ dKO, and MCK-miR-499 transgenic mice. Scale bar, 500 μm.

(**C**) Identification of myosin isoform content of Soleus, EDL, and TA muscles from wild-type, miR-208b$^{-/-}$/miR-499$^{-/-}$ dKO, and MCK-miR-499 transgenic mice by gel electrophoresis.
(**D**) The percentage of type I myofibers within soleus muscles of wild type, MyomiR mutant, and MCK-miR-499 transgenic mice was determined as shown in Panel B.
(**E**) βMHC mRNA levels in skeletal muscle of miR-208b$^{-/-}$/miR-499$^{-/-}$ dKO adult mice were detected by real time PCR. Loss of MyomiRs in skeletal muscle results in repression of βMHC.
(**F**) Expression of slow and fast myofiber genes in soleus, TA and EDL muscles of MCK-miR-499 transgenic mice compared to their level of expression in wild type muscles (set at a value of 1), as detected by real time PCR. Transgenic over-expression of miR-499 is sufficient to up-regulate slow myofiber genes and repress fast myofiber genes in soleus and EDL.
(**G**) WT (n = 4) and MCK-miR-499 transgenic (n = 5) mice were subjected to a regimen of forced running to exhaustion on a treadmill. The time to run to exhaustion of each mouse is shown. $p = 0.0039$.

by the reduced expression of slow β-MHC at the protein and mRNA levels (Fig. 3.4C and 3.4E), and by a concomitant increase in the expression of faster type IIx/d and type IIb myosin isoforms (Fig. 3.4C and Fig. 3.5A).

Conversely, forced expression of miR-499 under control of MCK regulatory elements, was sufficient to induce a complete conversion of all fast myofibers in soleus to a slow, type I phenotype (Fig. 3.4A, 3.4B, and 3.4C). Analysis of gene expression in the soleus by real-time PCR also demonstrated an induction of the slow fiber gene program in response to miR-499 overexpression (Fig. 3.4F). In the TA and EDL, which contain predominantly fast myofibers, we observed a pronounced induction of slow myofiber gene expression in MCK-miR-499 transgenic mice (Fig. 3.4F). Metachromatic ATPase staining of TA and EDL muscles from MCK-miR-499 transgenic animals also revealed conversion to

a slower myofiber type (data not shown). Separation of myosin isoforms by gel electrophoresis indicated a switch from fast type IIb fibers to slower type IIx/d and type IIa fibers in the EDL and TA of transgenic mice (Fig. 3.4C). This shift in fiber type was confirmed by real time PCR for fiber-type specific myosins (Figure 3.5B). In contrast, fast myofiber genes were repressed in both soleus and EDL muscles from MCK-miR-499 transgenic mice (Fig. 3.4F). Even more remarkable, when mice were subjected to a regimen of forced treadmill running, the miR-499 transgenic animals ran more than 50% longer than wild-type littermates, indicative of enhanced endurance resulting from the reprogramming of fast myofibers to a slower fiber type (Fig. 3.4G). We conclude that miR-208b and miR-499 redundantly program skeletal myofibers to a slow phenotype at the expense of fast myofibers.

MyomiR targets and mechanism

To begin to define the mRNA targets of MyomiRs that mediate their influence on myosin expression and myofiber phenotypes, we used targeting algorithms (TargetScan) to search for predicted targets that were evolutionarily conserved and encoded transcriptional regulators implicated in myofiber gene expression. In addition to the thyroid hormone receptor coregulator Thrap1,

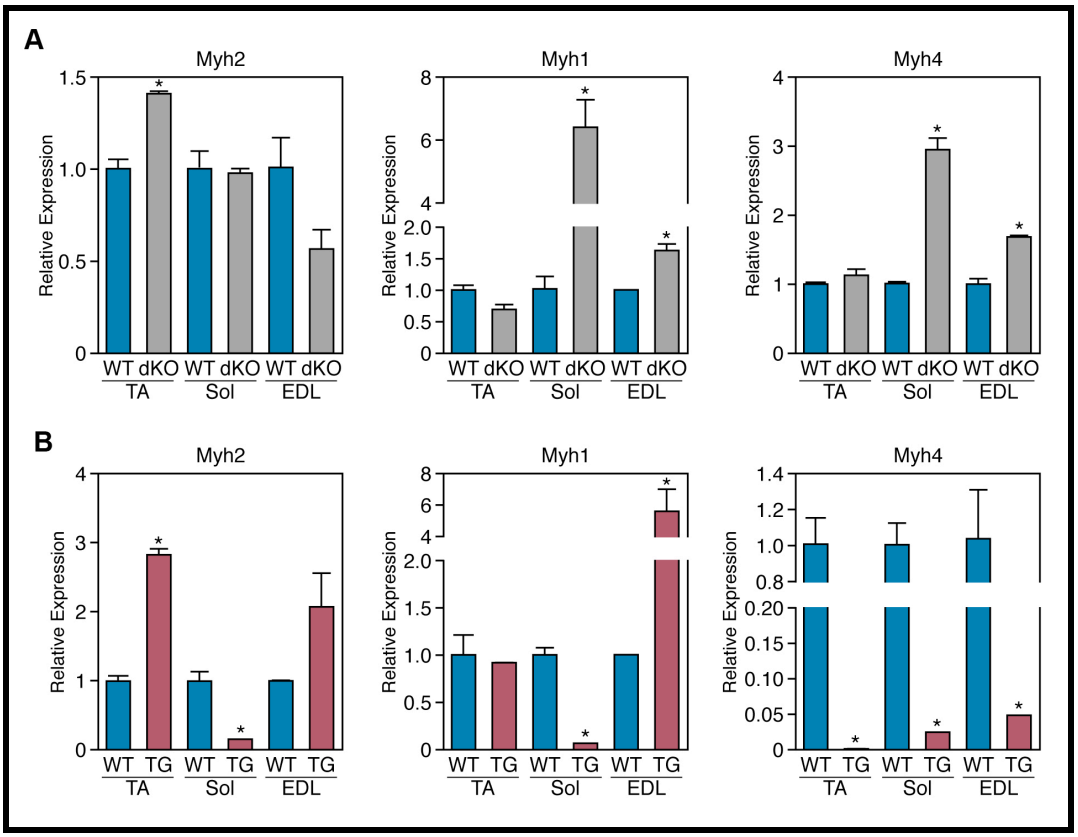

Figure 3.5. Analysis of myosin expression in skeletal muscle of MCK-miR-499 transgenic and dKO animals.
(**A**) Detection of fast skeletal myosin isoform expression in dKO skeletal muscle by real-time PCR.
(**B**) Detection of fast skeletal myosin isoform expression in MCK-miR-499 skeletal muscle by real-time PCR.

shown previously to be a target for repression by miR-208a in the heart (Callis et al., 2009; van Rooij et al., 2007), we identified several transcriptional repressors among the predicted targets of the MyomiRs (Figure 3.5). These include Sox6, Purb, and Sp3, each of which has been reported to repress *β-MHC* expression (Adolph et al., 1993; Azakie et al., 2006; Gupta et al., 2003; Hagiwara et al.,

2005; Hagiwara et al., 2007; Ji et al., 2007; Tsika et al., 2004; von Hofsten et al., 2008); and HP-1β, a corepressor of MEF2 (Zhang et al., 2002), which activates slow fiber gene expression (Wu et al., 2000).

The 3' UTR of Sox6 mRNA contains four evolutionarily conserved target sites for miR-499, one of which is also a predicted site for miR-208 (Figure 3.6). The 3' UTRs of Purb and HP-1b each contain single conserved predicted target sequences for miR-499 and miR-208a, while Sp3 contains a conserved miR-208 targeting sequence. We cloned the 3' UTRs of each of these predicted targets downstream of a luciferase reporter and assayed for repression by miR-208 and -499 in transfected COS cells. Expression of the MyomiRs repressed wild-type 3' UTR-luciferase reporter constructs, but had little effect on reporters containing 2 nucleotide mutations in the conserved targeting sequence (Fig. 3.7A). Similarly, wild-type luciferase reporter constructs were repressed in C2C12 cells as MyomiR expression increased over the course of differentiation, while mutated constructs displayed no change in activity (Fig. 3.7B and 3.7C). Consistent with previous results, the 3'UTR of Thrap1 displayed repression by both miR-208a and miR-499 (data not shown).

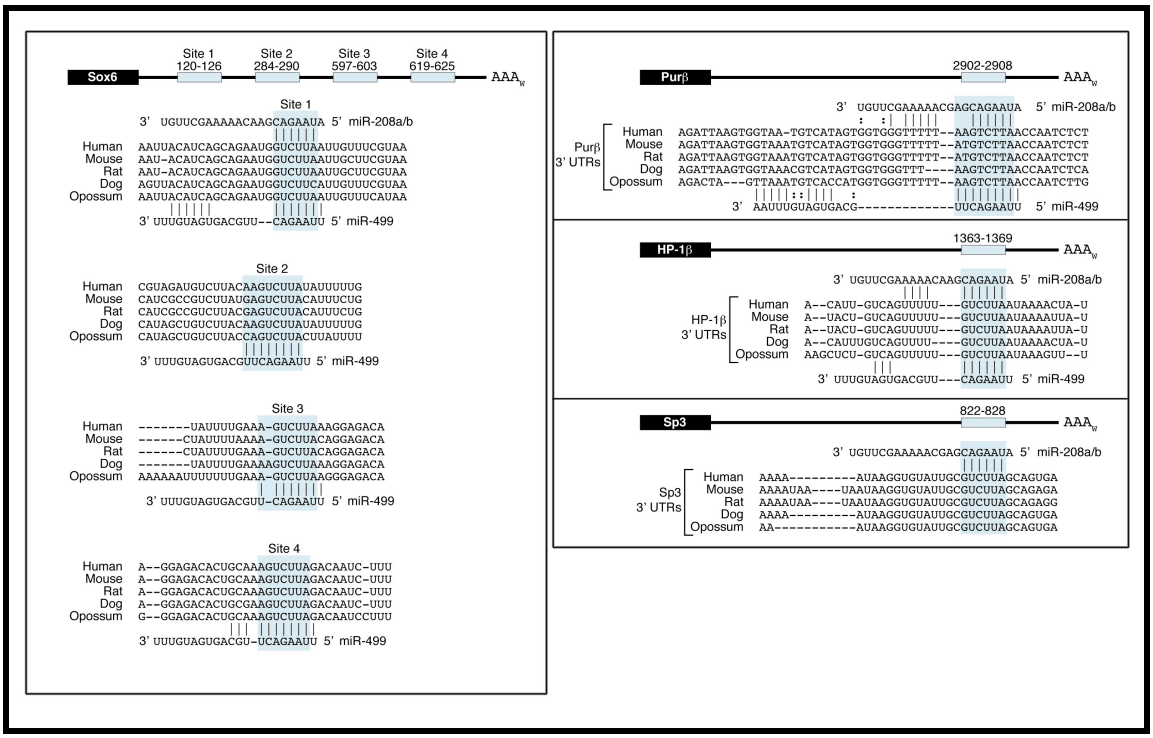

Figure 3.6. MyomiR target sites
Predicted targets of MyomiRs are shown along with the positions of target sequences in the 3' UTRs of mouse mRNAs.

To further validate the *Sox6* as a potential target of the MyomiRs, we compared the expression of *Sox6* transcripts in MyomiR null tissue. Sox6 mRNA levels were reduced in skeletal muscles of MCK-miR-499 transgenic mice, indicative of a destabilizing effect of miR-499 on Sox6 mRNA (Fig. 3.8A). Such down-regulation of Sox6 suggests that Sox6 mediates, at least in part, the increase in slow and decrease in fast myofiber gene expression in MCK-miR-499 transgenic mice, as shown in Figure 3.4F.

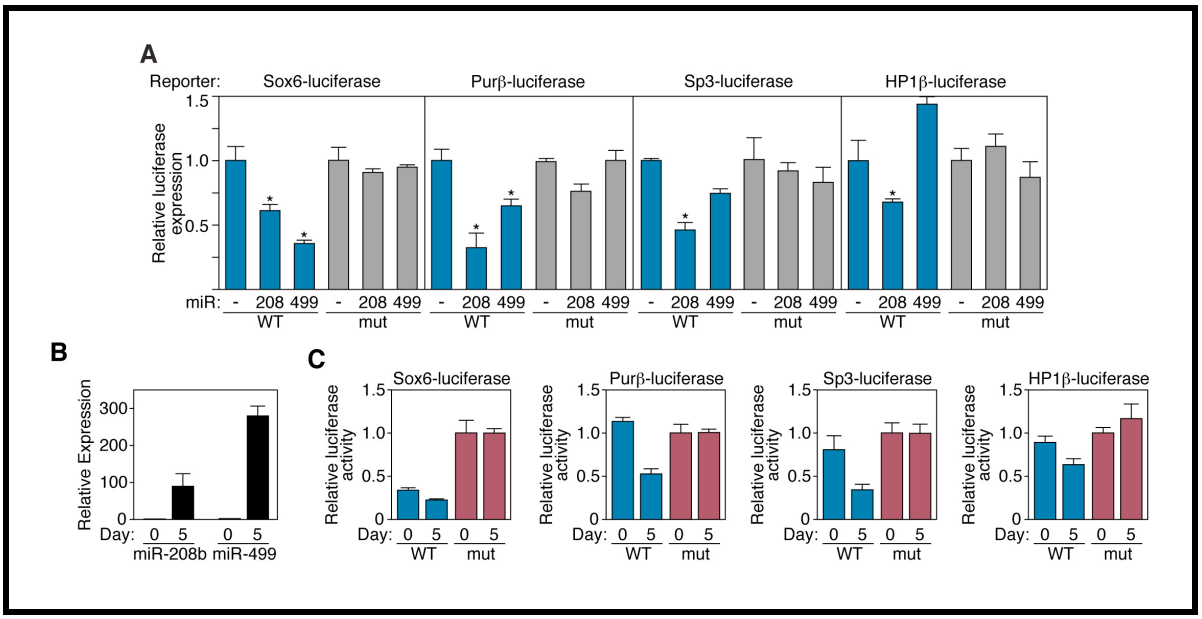

Figure 3.7. MyomiRs directly repress predicted target genes.
(**A**) Luciferase studies of predicted MyomiR target transcripts. Wild-type and mutant Sox6, Purβ, Sp3, and HP1β 3'UTRs were cloned into a luciferase reporter plasmid. These constructs were co-transfected into COS-1 cells with expression vectors for miR-208a or miR-499. Luminescence values were assayed forty-eight hours post transfection and were normalized to β-galactosidase activity.
(**B**) Expression of MyomiRs increases following C2C12 myoblast differentiation. Relative levels of miR-208b and miR-499 expression were detected by real-time PCR at days 0 and 5 of C2C12 differentiation.
(**C**) Wild-type, but not mutant luciferase reporter constructs are repressed by MyomiRs in C2C12 cells.

Transgenic expression of Sox6 phenocopies MyomiR gene deletions

To further validate Sox6 as potential mediator of MyomiR function, we generated MCK-Sox6 transgenic mice. MCK-Sox6 mice appeared normal at birth, however they demonstrated retarded growth at postnatal day 8 and ultimately died by 28 days of age. Analysis of multiple F0 transgenic animals revealed that over-expression of Sox6 in skeletal muscle strongly repressed *β*-

MHC and slow *Tnni1* transcript levels (Fig. 3.8B). Immunohistochemistry for β-MHC on skeletal muscle sections revealed a complete loss of type I fibers in MCK-Sox6 mice (Fig. 3.8C). Thus, over-expression of Sox6 at relatively modest levels (Figure 3.8B) was sufficient to evoke a myofiber phenotype similar to the MyomiR dKO mice. This result provides strong support for the conclusion that the transcriptional repressor Sox6, in part, mediates the actions of MyomiRs on slow myofiber gene expression.

In contrast, Sox6 did not activate the expression of fast *Tnni2* or *Tnni3* (Fig. 3.8B), as seen in miR-208b$^{-/-}$/miR-499$^{-/-}$ dKO mice. The latter findings suggest that Sox6 mediates the actions of miR-499 and miR-208b on the slow myofiber gene program, but other targets of these MyomiRs are required for the activation of fast myofiber genes.

Discussion

This work identifies microRNAs as novel regulators of the slow muscle gene program, and the MyomiR family as critical effectors of muscle contraction in the heart and skeletal muscle.

MicroRNA feedback loops

Myosin heavy chain is a key component of the sarcomere that generates contractile force. This study demonstrates that loci, encoding functional

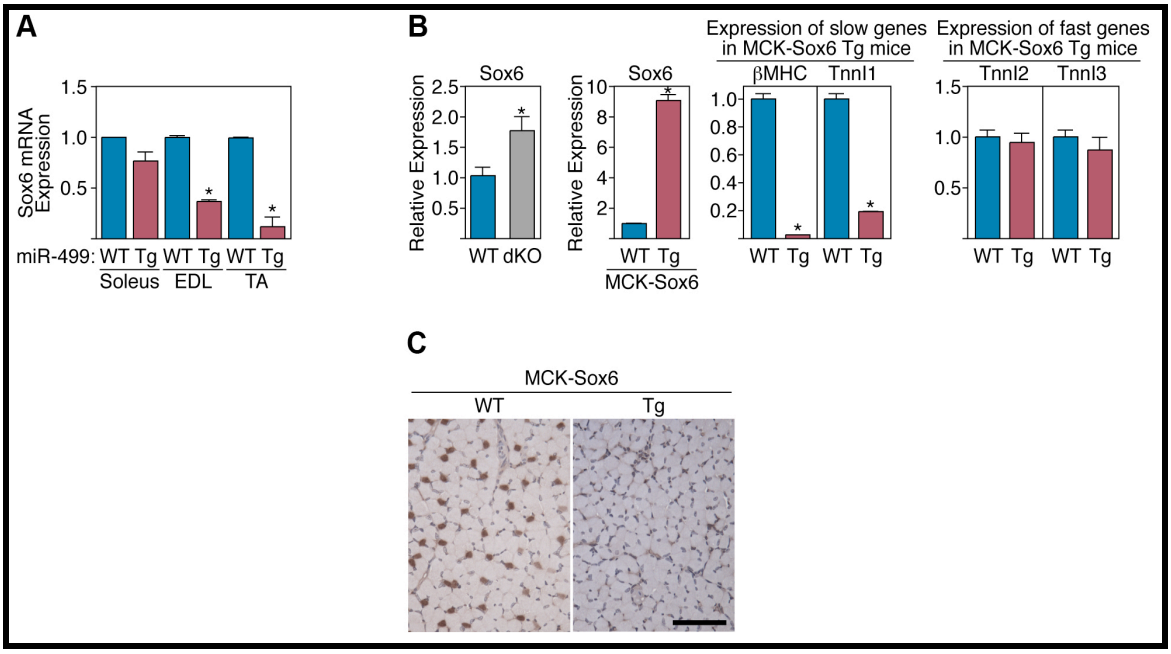

Figure 3.8. Sox6 mediates the actions of MyomiRs in skeletal muscle
(**A**) Real time PCR indicates Sox6 mRNA levels are depressed in skeletal muscle of MCK-miR-499 mice.
(**B**) Sox6 mRNA transcript is over-expressed in MyomiR dKO skeletal muscle. MCK-Sox6 transgenic mice exhibit repression of slow skeletal muscle genes and unaltered levels of fast skeletal troponin in skeletal muscle. Expression was measured by real time PCR in total hind limb muscle of MCK-Sox6 transgenic mice and wild type (WT) controls.
(**C**) Immunohistochemistry for Type I myosin (βMHC) in the hind limb of MCK-Sox6 transgenic mice indicates an absence of Type I fibers in the EDL of transgenic mice as compared to wild-type (WT) littermate controls. Scale bar, 100 μm.

slow myosin proteins, also express microRNAs that evoke other aspects of a slow contractile phenotype. Thus, the information generated by a single transcriptional event at the *Myh6*, *Myh7*, and *Myh7b* loci influences both contractile and

metabolic aspects of muscle phentoype. This positive feed forward system ensures that a stimulus that promotes slow myosin expression, such as increased intracellular calcium, effectively and completely regulates all aspects of the phenotype to elicit an adaptive response. Similar microRNA mediated regulatory loops have also been recently discovered. MiR-33 cooperates with its host gene SREBP to promote a cholesterologenic state within a cell by repressing cholesterol efflux (Najafi-Shoushtari et al., 2010), and miR-218, encoded within an intron of the ligand *Slit2*, ensures mutually exclusive ligand-receptor expression by antagonizing expression of the cognate Robo4 receptor.

MyomiR induced myofiber transitions

We have observed that manipulation of MyomiR levels in the soleus, TA, and EDL elicits a distinct shift towards the slow phenotype in each muscle. In addition to up-regulating *β-MHC*, transgenic expression of miR-499 primarily drives these muscles to shift one myofiber type slower in the sequential transition towards a slow myofiber phenotype(Pette and Staron, 1997). We hypothesize that divergent gene expression profiles, as well as different frequencies of muscle use between the soleus, TA, and EDL may be responsible for the distinct changes we observe in response to gain of MyomiR function. Further investigation of the mechanisms that confer differential responsse to the MyomiRs between muscle groups could uncover novel myofiber type regulatory mechanisms.

MyomiRs as common regulators of contraction in heart and skeletal muscle

Finally, this study demonstrates that miR-208b and miR-499 serve a function in skeletal muscle similar to that of to the closely related miR-208a in the heart. In cardiomyocytes, miR-208a is the dominant MyomiR that regulates the expression of the other member of the MyomiR family and slow contractile genes. In skeletal muscle, miR-499 and miR-208b are redundant, as loss of either individual microRNA does not effect myofiber type differentiation. It will be of great interest to determine if the identical effect of the MyomiRs on the contractile phenotype in heart and skeletal muscle results from a common set of downstream target genes, or if the pathways have diverged to regulate a unique set of targets in each tissue. Additionally, identification of the mechanism by which miR-208a has ascended to a dominant role over other MyomiRs in the heart could highlight the divergence of the MyomiR regulatory network between heart and skeletal muscle.

Methods

Gene expression analysis. Whole skeletal muscle was flash frozen in liquid nitrogen, and total RNA was isolated following tissue homogenization in Trizol(Invitrogen) according to manufacturers instructions. cDNA was generated by reverse transcription using random hexamer primers (Invitrogen). Gene

expression was measured by quantitative real time PCR either with purchased gene specific Taqman probes (ABI) or primers designed (see supplemental data) for SYBR green qPCR.

Generation of transgenic mice. A mouse genomic fragment flanking miR-499 was subcloned into a muscle-specific expression plasmid containing the MCK enhancer and human GH poly(A)+ signal (Sternberg et al., 1988). Genomic DNA was isolated from mouse tail biopsies and analyzed by PCR using primers specific for the human GH poly(A)+ signal.

Generation of miR-208b mutant mice. To generate the miR-208b targeting vector, a 4.9kb region (5' arm) extending upstream of the miR-208b coding region was ligated into the pGKneoF2L2dta targeting plasmid upstream of the loxP sites and the Frt-flanked neomycin cassette. A 3.5 kb fragment (3' arm) was ligated into the vector between the neomycin resistance and Dta negative selection cassettes. Targeted ES-cells carrying the disrupted allele were identified by Southern blot analysis with 5' and 3' probes. Three miR-208b targeted ES clones were identified and used for blastocyst injection. The resulting chimeric mice were bred to C57BL/6 to obtain germline transmission of the mutant allele.

Fiber-type staining. Soleus, GP, TA, and EDL muscles were isolated at 8 weeks of age and were embedded in a 3:1 ratio of Tissue Freezing Medium to gum tragacanth. Samples were flash frozen and sectioned on a cryostat-microtome. Metachromatic ATPase staining was performed as previously described (Ogilvie and Feeback, 1990).

Forced running. Forced treadmill running of 6 week old wild-type and MCK-miR-499 transgenic mice was performed as follows. Animals were trained on the treadmill (Colombus Instruments, 10% incline) for 5 minutes at 7m/min for two consecutive days. The following day mice were run at 8m/min for 30 minutes, then 9m/min for 15 minutes, followed by 10m/min for 15 minutes. Finally, speed was incrementally increased by 1m/min every 10 minutes until the mouse exhibited exhaustion. The end point was reached when a mouse received repeated electrical stimuli for greater than 5 seconds.

MHC electrophoresis. Myosin was isolated from skeletal muscle and run on glycerol-SDS-PAGE gels as previously described (Talmadge and Roy, 1993). Gels were stained with a silver nitrate staining kit(Biorad).

Cell culture, transfection and luciferase assays. A 300-500 bp genomic fragment encompassing the miR-208a, miR-499, miR-21 or miR-206 coding

region, were amplified by PCR and ligated into pCMV6. Full length 3' UTRs of Sox6, Sp3, HP1b, and PURβ were cloned into the pMiR-report vector (Ambion). Cell culture, transfection, and luciferase studies were performed as previously described (van Rooij et al., 2007), Mutations in the 3'UTRs alter the 2nd and 3rd nucleotides of the targeting sequence, and were genereated using QuickChange Lightning kit (Stratagene).

Immunohistochemistry. Tissue samples were fixed in 4% paraformaldehyde and embedded in paraffin for sectioning. Deparaffinized sections were permeabilized with 0.04% Pronase E, then blocked in 0.5% bovine serum albumin/5% normal goat serum in PBS. NOQ7.5.4D (1:16000) was used for primary detection of Type I myosin, and HRP-conjugated secondary (Sigma A8924) followed by DAB chromagen reaction were used for detection. Samples were then counterstained with hematoxylin.

Analysis of transgenic animals. Two F1 transgenic lines of MCK-miR-499, and 3 F0 transgenic MCK-Sox6 animals were analyzed in this study.

Statistical Analysis. All graphs represent mean values +/- SEM. Asterisk(*) represents p-value<0.05 as calculated by unpaired t-test.

Animal Care. All animal procedures were previously approved by the Institutional Animal Care and Use Committee at UT Southwestern Medical Center.

CHAPTER IV

REGULATION OF MUSCLE GENE EXPRESSION AND PERFORMANCE BY SOX6

Abstract

In response to physiological stimuli, skeletal muscle alters its myofiber composition to significantly affect muscle performance and metabolism. This process requires concerted regulation of myofiber specific isoforms of sarcomeric and calcium regulatory proteins that couple action potentials to the generation of contractile force. Here, we identify Sox6 as a fast myofiber enriched repressor of slow muscle gene expression *in vivo*. Mice lacking Sox6 specifically in skeletal muscle have an increased number of slow myofibers, elevated mitochondrial activity, and exhibit down regulation of the fast myofiber gene program, resulting in enhanced muscular endurance. In addition, microarray profiling of Sox6 knockout muscle revealed extensive muscle fiber type remodeling, and identified numerous genes that display novel fiber type enrichment. Sox6 directly represses the transcription of slow myofiber enriched genes by binding to conserved cis-regulatory elements. These results identify Sox6 as a robust regulator of muscle contractile phenotype and metabolism, and elucidate a mechanism by which

functionally related muscle fiber type specific gene isoforms are collectively controlled.

Introduction

The *Sry*-related HMG box (SOX) family of transcription factors is a large group of proteins with established roles in the regulation of gene expression during development and disease. Members of the SOX family are defined by the presence of an HMG box DNA-binding domain, of which they must share greater than 50% sequence homology (Bowles et al., 2000). This loose classification criteria has led to the identification of more than 30 *Sox* genes, which are further clustered into eight groups, A-H, based on their HMG domain sequence homology.

The SoxD sub-class is uniquely identified by the C-terminal localization of their HMG box, and the presence of an N-terminal coil-coiled dimerization domain. This group is composed of *Sox5*, *Sox6*, and *Sox13*, which exhibit dual functions as transcriptional activators or repressors (Lefebvre, 2002; Lefebvre et al., 1998). Sox5 and Sox6 are capable of regulating transcription of their target genes as homo- or heterodimers (Lefebvre et al., 1998), and have been shown to play redundant roles during chondrogensis *in vivo* (Smits et al., 2001). Sox6 null

mice exhibit failure to thrive and expire within 2 weeks following birth (Smits et al., 2001), however studies in these mice, as well as in zebrafish, have identified an important role for Sox6 in embryonic muscle development(Hagiwara et al., 2005; Hagiwara et al., 2007; von Hofsten et al., 2008).

In the present study, we investigate the function of Sox6 in adult skeletal muscle. We show that Sox6 is required for fast myofiber maintenance in adult muscle, as conditional loss of Sox6 leads to conversion of muscle to a slow myofiber phenotype, resulting in significant changes in skeletal muscle mechanics. We demonstrate that Sox6 regulation of muscle phenotype occurs independent of changes in other regulatory factors implicated in fiber type switching, such as PGC-1α and AMP-kinase (AMPK), and instead results from direct repression of a constellation of slow isoforms of sarcomeric and calcium regulatory proteins. Together, these data reveal an important role for Sox6 in the coordinated regulation of multiple properties of myofiber phenotype that profoundly effect muscle performance.

Results

Sox6 is enriched in fast myofibers

Previous work suggests a role for Sox6 in embryonic muscle differentiation, but the potential functions of Sox6 in adult muscle are unknown, therefore we asked if Sox6 displays differential expression between muscle fiber types in adult mice. Comparison of slow myofiber enriched soleus muscle to fast myofiber enriched tibialis anterior (TA) and extensor digitorum longus (EDL) by qPCR revealed that Sox6 mRNA is expressed approximately 3-fold higher in fast TA and EDL muscle groups (Figure 4.1A). To more thoroughly study the influence of fiber type on the expression of Sox6 within an individual muscle group, we utilized transgenic mice that express an active form of the phosphatase calcineurin under control of muscle creatine kinase (MCK) regulatory elements, which drives slow myofiber formation in skeletal muscle (Naya et al., 2000). Expression of Sox6 in slow myofiber enriched MCK-CnA TA muscle was reduced by approximately 50% when compared to WT TA by qPCR (Figure 4.1B). Based on these results, we conclude that Sox6 is more highly expressed in fast myofibers.

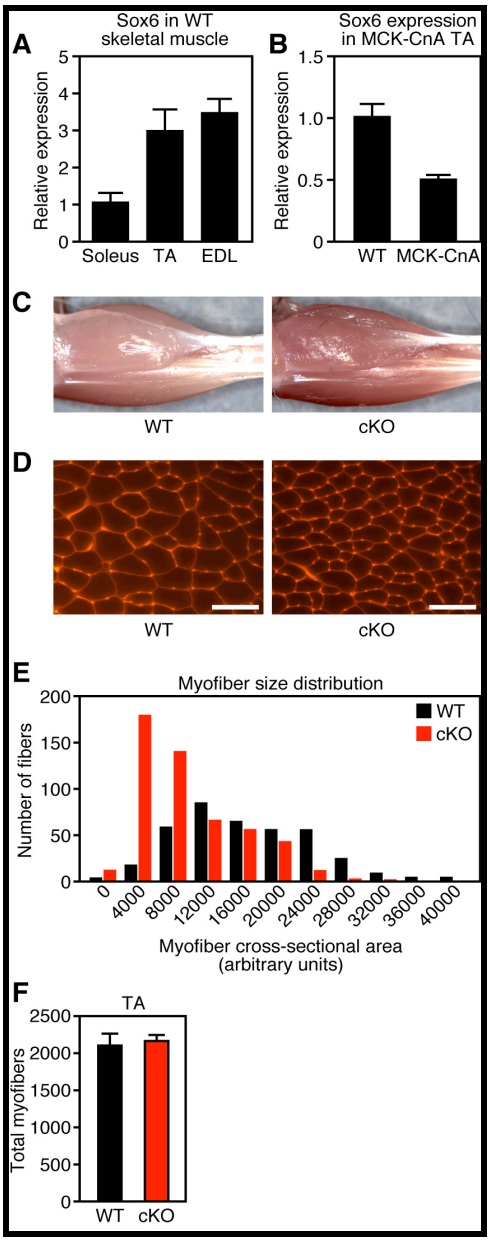

Figure 4.1. Sox6 is enriched in fast muscle fibers and affects gross muscle fiber morphology.
(**A**) Sox6 mRNA is enriched in muscle groups that predominantly contain fast myofibers (TA and EDL) compared to slow myofiber enriched muscle (soleus), as measured by qPCR.

(**B**) Sox6 expression levels are reduced by qPCR in slow fiber containing MCK-CnA transgenic TA muscle compared to WT fast TA muscle.
(**C**) Gross examination of adult Sox6 cKO hindlimb muscles demonstrates increased redness and a reduction in muscle size compared to WT control.
(**D**) Staining of myofiber cell membranes with wheat germ agglutinin indicates a reduction in myofiber size in Sox6 cKO TA muscle. Scale bars: 200 μm.
(**E**) Quantification of myofiber size following wheat germ agglutinin staining reveals an increase in the proportion of smaller myofibers and a reduction in the proportion of larger myofibers in Sox6 cKO TA muscle.
(**F**) Sox6 cKO and WT TA muscle contain a similar number of myofibers.

Loss of Sox6 alters myofiber appearance and morphology

To study the function of Sox6 in skeletal muscle, we bred mice conditionally targeted at the Sox6 locus (Dumitriu et al., 2006) with mice expressing Cre-recombinase in post-natal skeletal muscle under the control of MCK regulatory elements (Bruning et al., 1998). $Sox6^{f/f}$;MCK-Cre conditional knockout mice (henceforth referred to as Sox6 cKO) were born at mendelian ratios and appeared identical to WT littermate controls (data not shown). Analysis of Sox6 expression in 8-week old cKO mice by qPCR revealed a reduction in Sox6 transcript levels by 70% in TA and EDL muscles, and by 25% in soleus muscle (Figure 4.2A). By gross examination, hind limb musculature of adult Sox6 cKO mice was markedly darker and more red in color than that of WT littermates (Figure 4.1C).

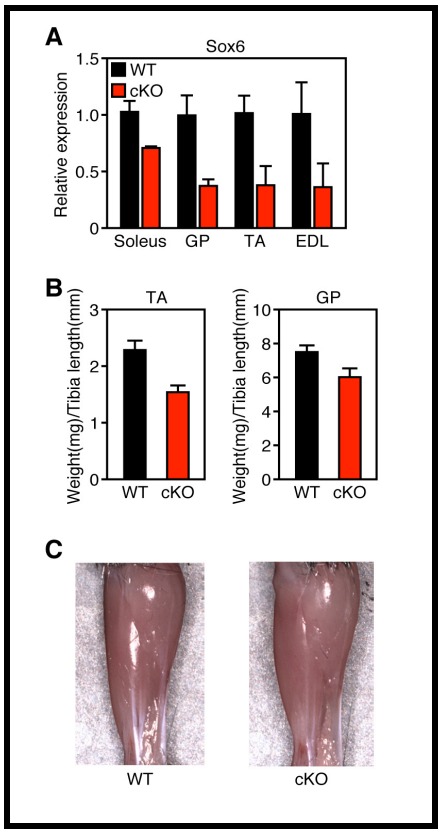

Figure 4.2. Reduced Sox6 expression and muscle mass in adult Sox6 cKO mice
(**A**) Measurement of Sox6 expression in 8 week-old WT and Sox6 cKO mice by real-time qPCR.
(**B**) Sox6 cKO TA and GP muscle from 8 week-old mice demonstrate a reduction in muscle mass.
(**C**) Grossly, WT and Sox6 cKO hind limb musculature appear identical at P10.

Furthermore, cKO muscle weighed less than WT controls (Figure 4.2B). Examination of myofiber cross-sectional area by histochemical staining revealed that fiber size distribution was altered in Sox6 cKO TA muscle, with a shift toward a reduced cross sectional area relative to WT (Figure 4.1D and 4.1E). Quantification of total myofiber number revealed that Sox6 cKO TA muscle

contained a comparable number of individual fibers to WT controls (Figure 4.1F), indicating that the decrease in Sox6 cKO muscle mass results solely from a reduction in myofiber size. Importantly, gross morphological changes in Sox6 cKO muscle were absent in young mice at stage P10 (Figure 4.2C, 4.4B, and 4.4C), suggesting that the observed phenotype in Sox6 cKO adult mice is not due to adverse effects on normal muscle development or early fiber type patterning.

Enhanced muscle performance in Sox6 cKO mice

The altered appearance of Sox6 cKO muscle is consistent with changes observed in endurance trained muscle (Holloszy and Booth, 1976), leading us to ask if muscle from Sox6 cKO mice displayed altered mechanical performance. EDL and soleus muscles were isolated from WT and Sox6 cKO mice, and physiological performance was assessed *ex vivo* in a muscle bath. Sox6 cKO soleus and EDL muscle generated stress comparable to WT controls over a range of stimulation frequencies (Figure 4.3A). Measurement of shortening velocity revealed that Sox6 cKO EDL, but not cKO soleus, had a reduced maximal shortening velocity compared to WT (Figure 4.3B).

We assayed muscle endurance by calculating the time to fatigue; measured as the length of time for a muscle to fall to a defined percentage of its initial force under constant stimulating frequency. Remarkably, the time to fatigue for cKO EDL muscle (50% of initial force) was 50% greater than WT muscle, indicating a

significant increase in cKO muscle endurance (Figure 4.3C). This pronounced improvement in physiological performance was also evident in the cKO soleus, which displayed a 100% increase in the time to fatigue (75% of initial force) (Figure 4.3C). Sox6 cKO EDL and soleus muscle also demonstrated improved recovery following fatigue (Figure 4.4D).

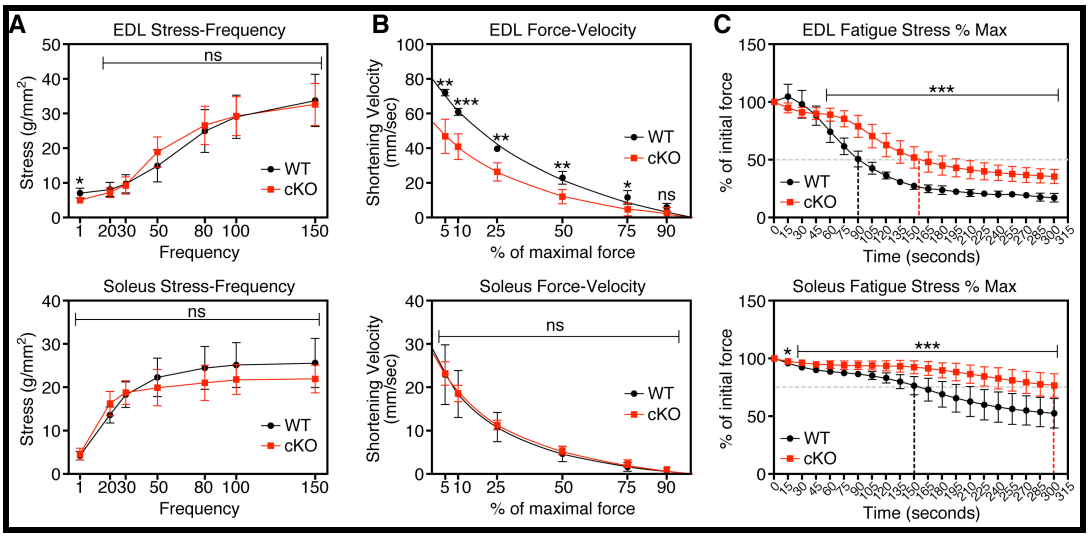

Figure 4.3. Altered physiological performance of Sox6 cKO muscle
(**A**) A stress-frequency plot of WT and Sox6 cKO EDL and soleus muscle reveals no difference in stress generation at various frequencies of stimulation.
(**B**) Measurement of the shortening velocity in WT and Sox6 cKO EDL and soleus muscle reveals a reduced maximal shortening velocity (y-intercept) in Sox6 cKO EDL, but not soleus. Lines represent curve fit of data points.
(**C**) Measurement of time to fatigue (i.e, to 50% of initial force; horizontal dashed line) for EDL muscle reveals an increase by 50% in Sox6 cKO EDL. Time to fatigue (i.e, 75% of initial force; horizontal dashed line) measurements for soleus muscle demonstrate an increase by 100%. These results indicate a significant improvement in Sox6 cKO muscle endurance. Vertical dashed lines indicate extrapolation of time to fatigue.
WT (n=4), Sox6 cKO (n=6). (*p<0.05, **p<0.01, ***p<0.001)

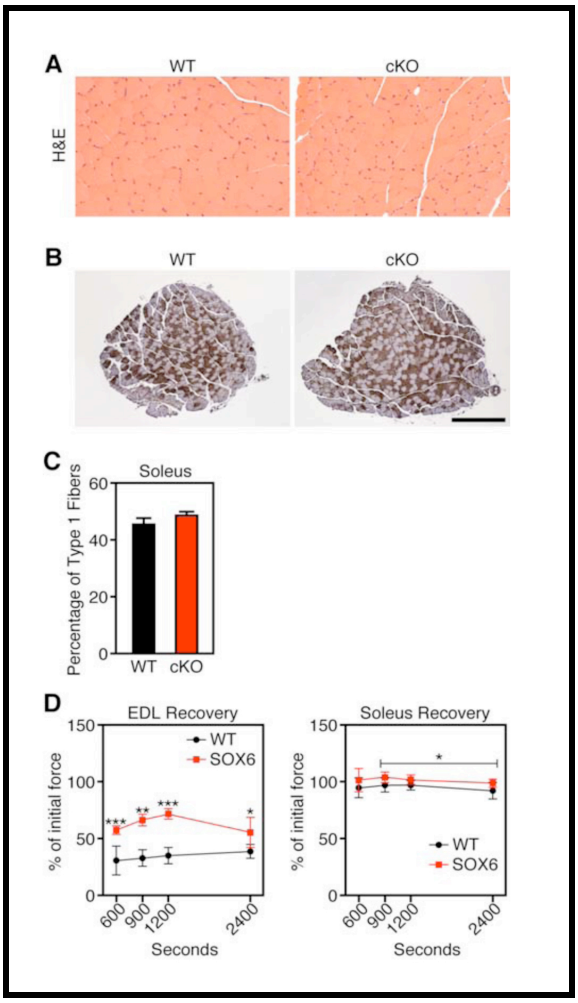

Figure 4.4. Normal fiber type distribution in post-natal Sox6 cKO muscle and improved recovery of adult cKO muscle

(**A**) H&E staining of WT and Sox6 cKO TA muscle reveals healthy looking muscle, with noticeably smaller myofibers in the Sox6 cKO TA at 8 weeks of age.

(**B**) Immunohistochemistry against Type I myosin in Sox6 cKO soleus displays normal fiber type patterning at P10. Slow fibers are stained brown. Scale bar: 400 μm.

(**C**) Quantification of Type I fibers in the soleus at P10 confirms preservation of WT fiber type patterning at P10.

(**D**) Sox6 cKO EDL and soleus generate a greater percentage of initial force than WT control muscle following fatigue, indicating enhanced recovery. Data points are a continuation of the plot from Figure 2C. (*p<0.05, **p<0.01, ***p<0.001)

Increased slow fibers in Sox6 cKO mice

The reduction in maximal shortening velocity and increase in muscle endurance observed in Sox6 cKO skeletal muscle led us to investigate muscle fiber type composition in these mice. Immunohistochemistry against type I slow myosin (β-myosin heavy chain) revealed a dramatic increase in the number of slow myofibers in several muscle groups from Sox6 cKO mice (Figure 4.5A). Quantification of the transcript encoding slow type I myosin, *Myh7*, by qPCR showed strong up-regulation in both fast and slow muscle groups of Sox6 cKO mice (Figure 4.5B). Similarly, analysis of muscle myosin isoform content by gel electrophoresis demonstrated that WT soleus was composed of 50% type I myosin, while the Sox6 cKO soleus contained nearly 100% slow type I myosin (Figure 4.5C). Sox6 cKO TA and EDL myosin electrophoretograms showed the presence of a band representing slow type I myosin, while this band was absent in WT TA and EDL samples (Figure 4.5C). In addition, Sox6 cKO TA and EDL lanes showed a shift from predominant expression of type IIb myosin, the fastest myosin isoform, towards expression of slower type IIa and IIx/d fast myosins. These changes in fast myofiber content were also evident by qPCR analysis of fast myosin isoform mRNA expression (Figure 4.5D).

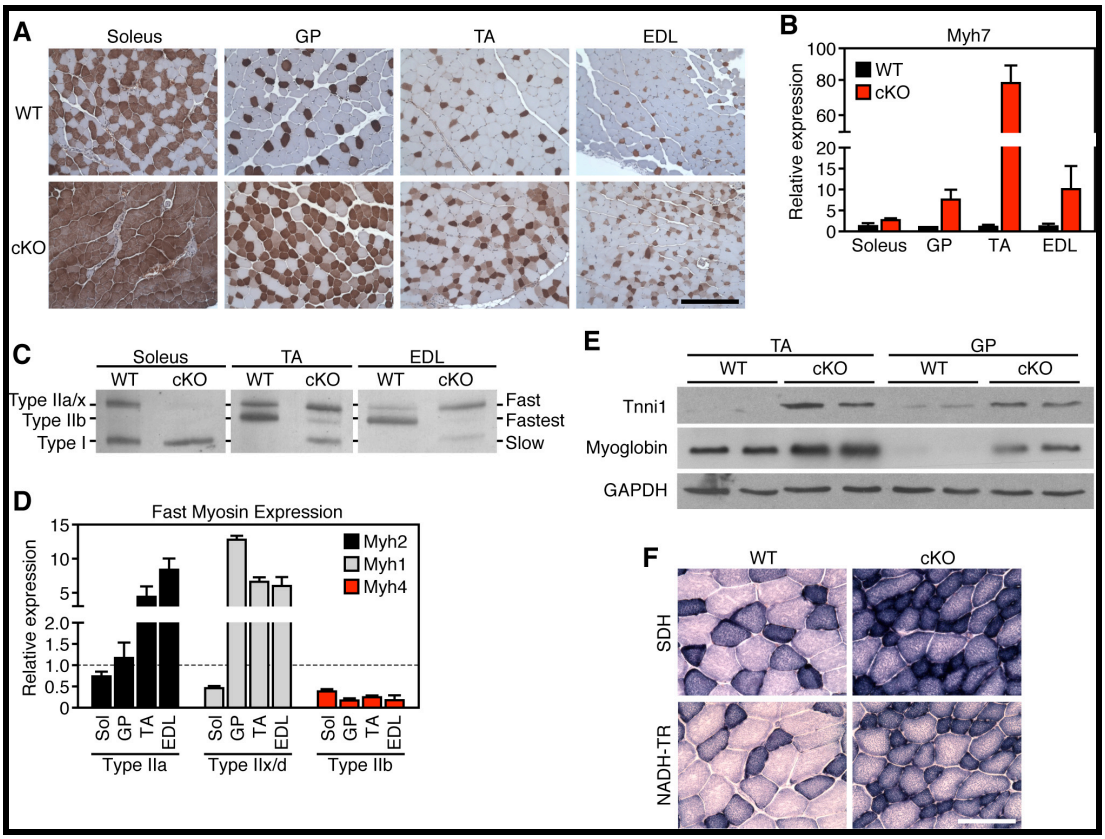

Figure 4.5. Increased slow myofibers and mitochondrial activity in Sox6 cKO mice

(**A**) Immunohistochemistry directed against type I slow myosin indicates an increase in slow myofibers in all muscle groups from Sox6 cKO mice at 8 weeks of age. Slow myofibers are stained brown. Scale bar: 400 μm.

(**B**) Measurement of *Myh7*, encoding type I slow myosin, by qPCR reveals significantly increased expression in Sox6 cKO muscle.

(**C**) Separation of myosin isoforms by gel electrophoresis reveals increased type I myosin in soleus, TA, and EDL muscle from Sox6 cKO mice. In addition, a switch from type IIb to type IIa/x fibers is evident in cKO TA and EDL.

(**D**) Sox6 cKO mice display altered expression of fast myosin isoforms compared to WT by qPCR.

(**E**) Western blots for slow skeletal troponin(Tnni1) and myoglobin demonstrate robust up-regulation of these proteins in TA and GP muscle from Sox6 cKO mice.

(**F**) Sox6 cKO TA muscle demonstrates increased succinate dehydrogenase(SDH) and NADH dehydrogenase(NADH-TR) enzymatic staining, consistent with an increase in mitochondrial activity in Sox6 cKO myofibers. Scale bar: 200 μm.

Next, we asked whether other slow myofiber specific genes might be regulated in Sox6 cKO mice. By western blot, we observed that the slow skeletal muscle specific troponin isoform, TNNI1, and slow muscle enriched myoglobin were both strongly up-regulated in cKO muscle (Figure 4.5E). We also compared the mitochondrial activity of muscle from Sox6 cKO mice to littermate controls. Sox6 cKO mice displayed higher levels of succinate dehydrogenase (SDH) and NADH dehydrogenase (NADH-TR) activity-dependant staining, indicating increased mitochondrial activity (Figure 4.5F). The up-regulation of slow myofiber specific gene expression, as well as the heightened mitochondrial activity in Sox6 cKO skeletal muscle, denotes a substantial increase in the number of slow type I myofibers.

Microarray profiling of Sox6 mice reveals extensive fiber type switching and novel myofiber specific gene expression

To more thoroughly analyze the changes that result from loss of Sox6 in skeletal muscle, we performed microarray analysis on mRNA isolated from WT and Sox6 cKO TA muscle. Of particular interest, microarray profiling revealed antithetical regulation of fiber type specific isoforms of sarcomeric components and ion channels involved in excitation-contraction coupling (Table 4.1). Gene ontology analysis of transcripts regulated by more than 2-fold in Sox6 cKO TA demonstrated significant enrichment of genes known to function in skeletal and

Table 4.1. Opposing regulation of fast/slow myofiber programs in Sox6 cKO TA muscle.

Component	Fast Isoform	Fold Change	Slow Isoform	Fold Change
Myosin heavy chain	MYH4	**0.16**	MYH7	**4.18**
Myosin light chain	MYL1	**0.51**	MYL2	**31.53**
Na/K ATPase	ATP1B2	**0.23**	ATP1B1	**1.96**
Troponin T	TNNT3	**0.72**	TNNT1	**8.20**
Actinin	ACTN3	**0.75**	ACTN2	**1.74**
Actin	ACTA1	**0.73**	ACTC1	**10.87**
Sarcoplasmic calcium channel	ATP2A1	**0.88**	ATP2A2	**13.93**

cardiac muscle contraction, as well as genes involved in various metabolic processes that differ between muscle fiber type (Figure 4.6C and 4.6D).

Given these robust changes in fiber type specific gene expression, we next investigated if Sox6 cKO mice could be used as a tool to identify new myofiber enriched genes. We generated a heat map depicting the most highly regulated genes in Sox6 cKO TA muscle (Figure 4.6A), and identified 26 genes with no known association with muscle fiber type or muscle function. We next analyzed muscle fiber type associated expression of these 26 genes in WT mice by comparing their expression in soleus and TA muscle by qPCR (Figure 4.6B). Cross referencing these data sets, we determined that *Rspo3* (*Thds2*), *Lrrn1, Lrba, DUPD1* and *Psat1* displayed slow myofiber enriched expression, while *Zmynd17, Smox, Kcnc4,* and *Mod1* demonstrated elevated expression in fast myofibers (Figure 4.6B). The transcripts *Sv2b and Chrna1*, encoding a neuron specific synaptic vesicle glycoprotein and the nicotinic cholinergic receptor, were also up-

regulated in slow muscle, potentially reflecting an increase in the number of neuromuscular junctions in Sox6 cKO TA and WT soleus muscle.

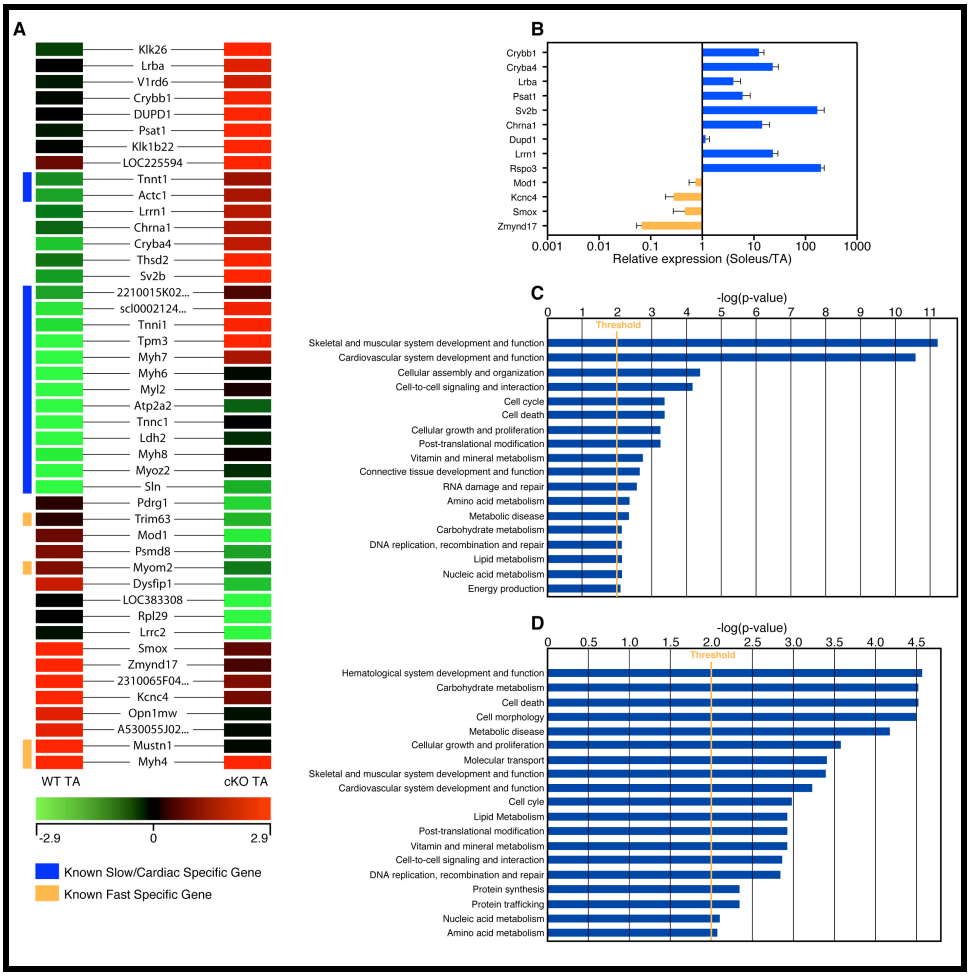

Figure 4.6. Microarray and gene ontology analysis of Sox6 cKO muscle
(**A**) Heat map analysis of genes regulated >5-fold in Sox6 cKO TA by microarray. Transcripts enriched in fast or slow myofibers are noted. 26 of 49 regulated genes have no known fiber type specificity or function in skeletal muscle.
(**B**) 13 transcripts from the microarray heatmap (Figure 4A) display novel fiber type enrichment in WT mice by comparison of expression in slow soleus muscle relative to WT fast TA muscle by qPCR.
(**C**) Gene ontology analysis of all genes up-regulated by 2-fold in Sox6 cKO TA muscle reveals significant enrichment of genes involved in muscle function and metabolism.

(**D**) Gene ontology analysis of all genes down-regulated by 2-fold in Sox6 cKO TA muscle indicates enrichment of genes critical for muscle structure/function and myofiber metabolism.

Sox6 directly represses expression of slow contractile and calcium handling genes

To elucidate the mechanism by which Sox6 regulates myofiber specific gene expression, we examined the possibility that Sox6 regulates factors known to promote slow myofiber gene expression. Pgc-1α, a transcriptional co-activator sufficient to drive slow fiber formation, was not changed in Sox6 cKO muscle as detected by western blot (Figure 4.7A). Additionally, levels of phosphoylated AMPK, a key metabolic regulator of muscle fiber transitions in response to endurance exercise(Rockl et al., 2007), were unchanged in cKO muscle (Figure 4.7B).

The strong increase in slow muscle fiber gene expression in Sox6 cKO mice, as well as the enrichment of Sox6 mRNA in fast myofibers led us to hypothesize that Sox6 acts as a direct repressor of slow myofiber gene expression. A search for the consensus Sox6 binding motif, AACAAT (Connor et al., 1995), near the loci of genes significantly regulated in cKO TA muscle by microarray identified conserved potential binding sites proximal to Myl2, Myl3, Myh1, Myh7, and ATP2a2 (Fig 4.8A and 4.7E). These loci encode slow muscle specific regulatory and essential myosin light chains (Myl2 and Myl3), a slow and

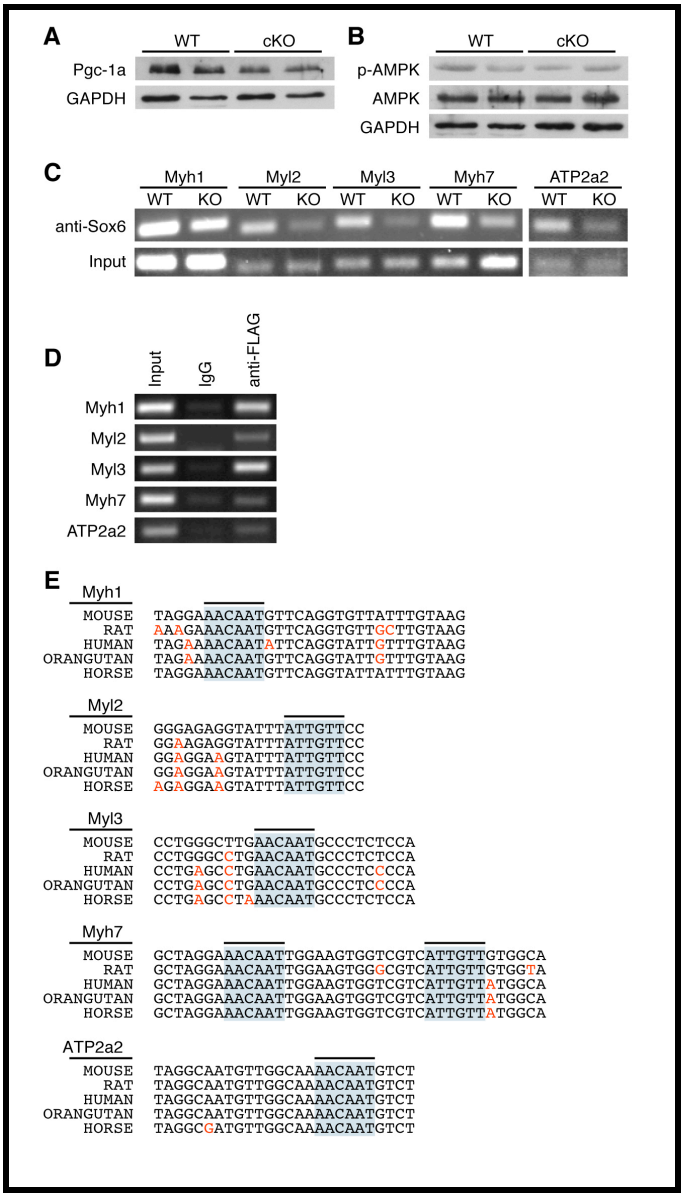

Figure 4.7. Absence of slow fiber signals and ChIP analysis of Sox6 targets in Sox6 cKO mice.

(**A**) PGC-1α expression is not altered in adult Sox6 cKO TA muscle as detected by western blot.

(**B**) Phosphorylated and total AMP-kinase levels are not changed in adult Sox6 cKO TA muscle compared to WT by western blot.

(**C**) Semi-quantitative PCR analysis of anti-Sox6 ChIP chromatin from WT and cKO TA samples at loci containing conserved Sox6 consensus binding sequences.

(**D**) Semi-quantitative PCR analysis of ChIP chromatin immunoprecipitated with anti-FLAG antibody and IgG negative control from FLAG-Sox6 transfected C2C12 cells. (**E**) The Sox6 binding motifs upstream of 5 target loci are strongly conserved among mammals.

intermediate isoform of myosin heavy chain (Myh7 and Myh1, respectively), and the slow fiber specific isoform of the sarcoplasmic reticulum Ca^{2+} uptake channel SERCA (ATP2a2 or SERCA2). To determine if Sox6 is present at these loci *in vivo* we performed chromatin immunoprecipitation (ChIP) assays from WT and Sox6 cKO TA muscle with an antibody directed against Sox6. Both qPCR and semi-quantitative RT-PCR analysis of ChIP chromatin indicated that Sox6 bound to all 5 loci in WT TA muscle, but was largely absent in Sox6 cKO TA (Figure 4.8B and Figure 4.7C). ChIP analysis of FLAG-epitope tagged Sox6 in C2C12 myoblasts yielded similar results (Figure 4.7D). In addition, gel shift analysis of the Sox6 consensus binding sites at all 5 loci revealed that Sox6 specifically bound to these DNA sequences *in vitro* (Figure 4.8E and 4.8F). In support of Sox6 acting as a transcriptional repressor at these loci, transcript levels of *Myl2*, *Myl3*, *Myh1*, *Myh7*, and *ATP2a2* were all increased in TA muscle from Sox6 cKO mice (Figure 4.8C). Conversely, in transgenic mice that over-express Sox6 specifically in skeletal muscle (van Rooij et al., 2009), *Myl2*, *Myl3*, *Myh1*, *Myh7*, and *ATP2a2* mRNA transcripts were all strongly decreased (Figure 4.8D). From these results, we conclude that Sox6 directly binds to loci encoding slow muscle fiber enriched genes and effectively represses their transcription.

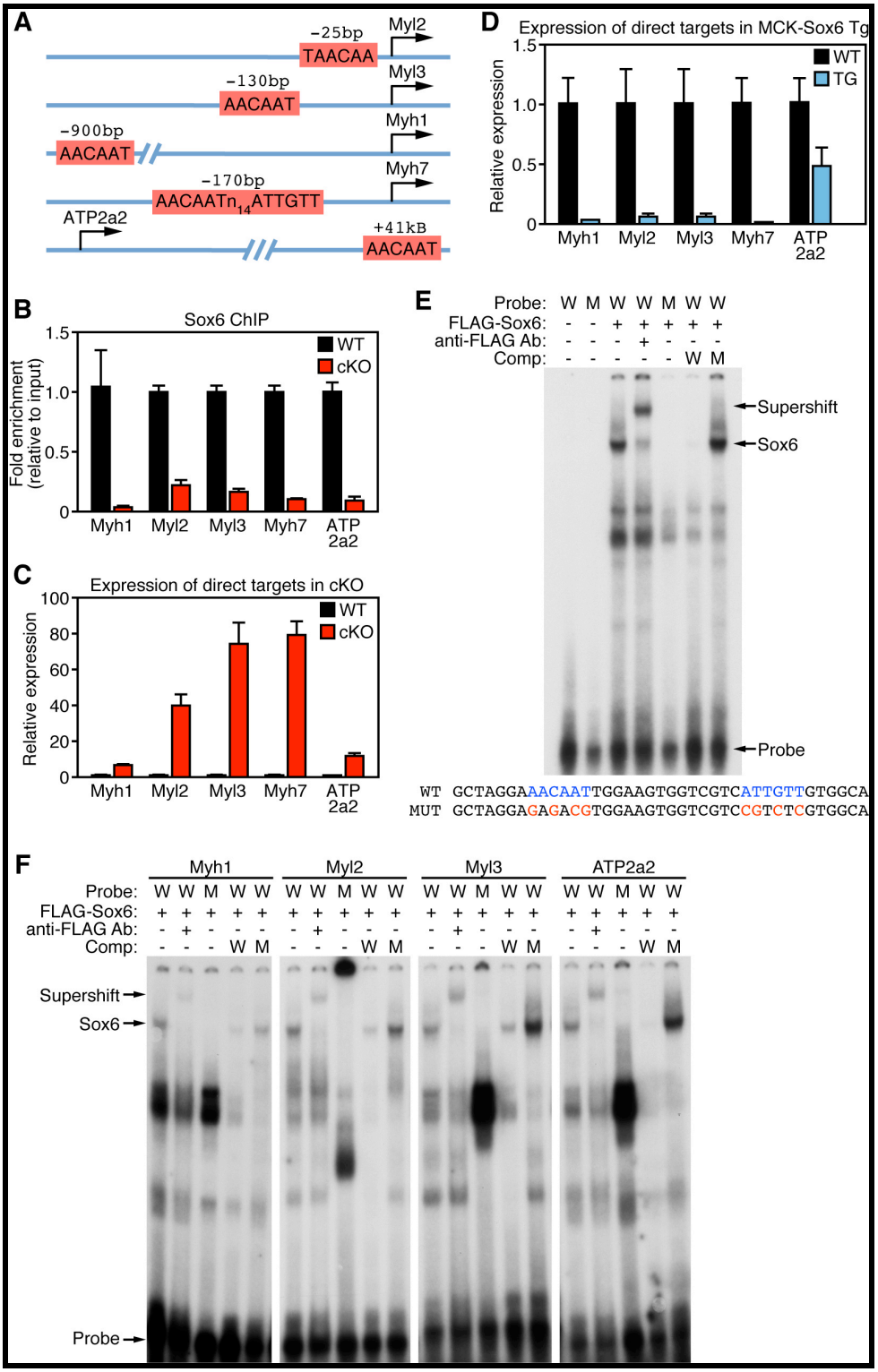
A
-25bp
TAACAA
Myl2
-130bp
AACAAT
Myl3
-900bp
AACAAT
Myh1
-170bp
AACAATn14ATTGTT
Myh7
ATP2a2
+41kB
AACAAT
B
Sox6 ChIP
Fold enrichment (relative to input)
WT
cKO
Myh1
Myl2
Myl3
Myh7
ATP 2a2
C
Expression of direct targets in cKO
Relative expression
D
Expression of direct targets in MCK-Sox6 Tg
WT
TG
E
Probe:
FLAG-Sox6:
anti-FLAG Ab:
Comp:
Supershift
Sox6
Probe
WT GCTAGGAAACAATTGGAAGTGGTCGTCATTGTTGTGGCA
MUT GCTAGGAGAGACGTGGAAGTGGTCGTCCGTCTCGTGGCA
F
Myh1
Myl2
Myl3
ATP2a2
Probe:
FLAG-Sox6:
anti-FLAG Ab:
Comp:
Supershift
Sox6
Probe

Figure 4.8. Sox6 is a direct repressor of slow myofiber genes
(**A**) Schematic representation of highly conserved Sox6 consensus binding motifs found near loci encoding slow fiber enriched genes.
(**B**) Sox6 chromatin immunoprecipitation assay (ChIP) reveals that all 5 loci are bound significantly more by Sox6 in WT TA muscle compared to Sox6 cKO TA negative control tissue.
(**C**) Direct Sox6 target genes are up-regulated in TA muscle from Sox6 cKO mice as measured by qPCR.
(**D**) Sox6 target gene transcripts are reduced in hindlimb muscle from MCK-Sox6 transgenic mice as measured by qPCR.
(**E**) Gel shift analysis of the palindromic Sox6 binding site upstream of the Myh7 locus. Sox6 binds wild-type (W), but not mutant (M) consensus binding sequence. The Sox6 binding complex is super-shifted with addition of α-FLAG antibody.
(**F**) Gel shift analysis of single Sox6 binding sites near loci for Myh1, Myl2, Myl3, and ATP2a2 reveals that Sox6 can bind to consensus binding sites *in vitro*.
(**G**) Our data suggests a model by which Sox6 represses multiple contractile genes that collectively contribute to slow muscle fiber contractile properties.

Discussion

In this work, we demonstrate an essential role for the transcription factor Sox6 in post-natal muscle fiber type differentiation, and consequently, muscle performance and metabolism. We show that mice lacking Sox6 in skeletal muscle display an increased number of slow muscle fibers and exhibit significantly improved endurance in response to mechanical workload. These changes result, at least in part, from a loss of transcriptional repression by Sox6 at loci encoding components of the contractile apparatus and calcium storage machinery that are specific for slow skeletal muscle.

Our data suggests that Sox6 is a regulator of muscle fiber type specification that acts in parallel to or downstream of PGC-1α and AMPK to induce slow myofiber formation. Additional experiments are necessary to elucidate the regulatory hierarchy that affects Sox6 function, however, our results are consistent with Sox6 as a target effector of the MyomiR regulatory network, which is sufficient, and partially required for slow myofiber formation(van Rooij et al., 2009).

In addition to the regulation of opposing myofiber specific gene profiles, muscle fiber type remodeling requires regulation of a broad spectrum sarcomeric components that function in concert to effect contraction. Here, we find that Sox6 regulates Myh7, Myh1, Myl3, and Myl2, that together form the thick filament myosin motor, and the slow muscle specific, ATP dependent, sarcoplasmic

reticulum Ca^{2+} uptake channel ATP2a2. Thus, Sox6 regulates both sarcomeric and calcium regulatory components that contribute to the contractile properties of slow myofibers. Further studies are needed to investigate if other sarcomeric proteins that affect the dynamics of muscle contraction, such as troponins and actins, are also directly regulated by Sox6. Additionally, identification of Sox6 targets that promote oxidative metabolism in slow myofibers would further our understanding of how metabolic and contractile properties of muscle fibers are co-regulated.

This study raises several important questions regarding the function of Sox6 in skeletal muscle. Previous *in vivo* loss-of-function studies of Sox6 have demonstrated significant functional overlap with the related SoxD family member Sox5 (Smits et al., 2001). Sox5 is highly enriched in human cardiac and skeletal muscle tissue (Ikeda et al., 2002), indicating potentially overlapping roles for Sox5/6 in the regulation of myofiber phenotype. Furthermore, while we demonstrate transcriptional repression of slow myofiber genes by Sox6, the possibility that Sox6 also plays an opposing role as a direct transcriptional activator of fast myofiber specific gene expression necessitates further inquiry.

The phenotype of the Sox6 cKO mouse exhibits a shift in both contractile and metabolic characteristics of the slow myofiber gene program. It is intriguing that the direct Sox6 targets identified in this study are all sarcomeric genes that control contraction. A recent study performed ChIP-Seq in myoblasts and

identified a similar set of slow, sarcomeric Sox6 target genes (An et al., 2011). Therefore, the extent to which the increase in oxidative metabolism in Sox6 cKO is directly mediated by loss of Sox6, or is influenced through indirect mechanisms is unclear.

Finally, the mechanisms by which Sox6 mediates transcriptional repression of target genes in skeletal muscle unknown. During oligodendrocyte development, Sox5 and Sox6 directly compete with the binding of the transcriptional activator Sox9 to cis-regulatory elements upstream of genes important for oligodendrocyte maturation (Stolt et al., 2006). In erythrocytes, SOX6 interacts with BCL11A to induce silencing of the fetal (γ) hemoglobin locus, and activate the transcription of adult (β) hemoglobin (Xu et al., 2010). Identification of SOX6 binding partners in skeletal muscle would potentially provide insight into the repressive mechanism. Additionally, bioinformatic analysis of nearby conserved cis-regulatory elements in Sox6 enhancers could identify other factors that cooperate with SOX6 to regulate gene expression.

Methods

MHC electrophoresis. Myosin was isolated from skeletal muscle and run on glycerol-SDS-PAGE gels as previously described (Talmadge and Roy, 1993).

SDH and NADH-TR Staining. Fresh frozen sections were incubated in 0.2 M phosphate buffer (pH 7.6) containing sodium succinate and NBT for 60 minutes at 37°C (SDH) or in 0.05 M TRIS buffer (pH 7.6) containing NADH and NBT for 30 minutes at 37°C (NADH-TR). Staining was then cleared with acetone and preserved with aqueous mounting medium.

Gel shift assay. Full length Sox6 cDNA was cloned from skeletal muscle and placed into pcDNA3.1 vector containing N-terminal FLAG tag. TnT *in vitro* translation (Promega) was used to generate tagged Sox6 protein. Double stranded gel shift probes were radioactively labeled with ATP[γ-^{32}P] by PNK and incubated with Sox6 protein in the presence or absence of cold competitor probes at room temperature. Mouse anti-FLAG antibody(Sigma) was used to supershift. Samples were resolved on a 5% native PAGE gel.

Quantification of myofiber size and number. Frozen sections were fixed in 100% ethanol and stained with Alexa594-conjugated wheat germ agglutinin (Invitrogen) at a concentration of 50μg/mL. Fibers were measured and counted using ImageJ software.

Statistical Analysis. All experiments represent an n=3 for WT and Sox6 cKO samples unless otherwise stated. All graphs represent mean values +/- SEM.

Animal Care. All animal procedures were previously approved by the Institutional Animal Care and Use Committee at UT Southwestern Medical Center and at Virginia Tech.

Muscle Bath Measurements. Mice were deeply anesthetized (2 mg xylazine-20 mg ketamine per 100 g of body mass, i.p.), fast-twitch extensor digitorum longus (EDL) and slow-twitch soleus muscles were excised, and non-absorbable silk surgical suture was tied to the proximal and distal myotendinous junctions. Muscles were incubated at 30ºC in an oxygenated (95% O_2-5% CO_2) physiological salt solution (PSS; pH 7.6 containing in mM: 120.5 NaCl, 4.8 KCl, 1.2 $MgSO_4$, 20.4 $NaHCO_3$, 1.6 $CaCl_2$, 1.2 NaH_2PO_4, 10.0 dextrose, 1.0 pyruvate) as previously described (Grange et al., 2002; Wolff et al., 2006). To obtain the contractile properties, muscles were fixed between a clamp and arm of a dual-mode servomotor system (300B, Aurora Scientific) at a resting tension (L_o) of 1.0 g. Muscle activation was provided by computer-generated electrical stimulation delivered through closely flanking platinum electrodes. EDL and soleus muscles were maintained at L_o by a stepper motor. The servomotor arm, stepper motor, and electrical stimulation were controlled by Dynamic Muscle Control software

(DMC Version 4.1.6, Aurora Scientific) to obtain the position and force output data from the activated muscles (Wolff et al., 2006).

The protocol to obtain contractile properties consisted of 5 steps: (1) a pre-twitch and tetanus, followed by a 10 min rest at L_o; (2) a stress frequency protocol, followed by a 5 min rest at L_o; (3) a force-velocity protocol, followed by a 5 min rest at L_o; (4) a fatigue protocol; and (5) a fatigue recovery protocol. In step 1, muscles were subjected to three isometric twitches and tetani (150 Hz) spaced 1 minute apart. In step 2, the muscle was subjected to stimulation at frequencies of 1, 30, 50, 80, 100, and 150 Hz, with each stimulation lasting 1 second and separated by 1 minute. For step 3, maximal force output was determined from the 150 Hz tetanus determined at the end of step 2, and then corresponding shortening velocities were determined after-loaded isotonic contractions of 5%, 10%, 25%, 50%, 75%, and 90% of this maximal force, using a tetanic afterload protocol (Brooks and Faulkner, 1988). The force-velocity relationship was established by plotting the mean isotonic loads (% maximum force in g) against the peak shortening velocities (mm/s) and fitting with the Hill equation (GraphPad Prism, GraphPad Software, Inc) as previously described (Grange et al., 1995). The maximum shortening velocity for each muscle (i.e., V_{max}) was determined by solving the fitted Hill equation at zero load load (Brooks and Faulkner, 1988). In step 4, muscles were fatigued by stimulating at 60 Hz (EDL) or 100 Hz (soleus) for 800 ms, once every 5 seconds, for a total of 300

seconds, as previously described (Call et al., 2008). Finally, in step 5, fatigue recovery was determined by collecting muscle force at 60 Hz (EDL) or 100 Hz (soleus) at 5, 10 15, and 30 minutes post-fatigue. At the conclusion of the protocols, muscle length was determined to the nearest 0.1 mm with a micrometer, muscle mass determined to the nearest 0.1 mg using an A-200D electronic analytical balance (Denver Instruments, Denver, Colorado) and then the muscle was snap frozen in liquid nitrogen for subsequent analysis.

Microarray analysis. Pooled triplicate samples of total RNA were analyzed on an illumina MouseWG-6 v2.0 BeadChip. Relative fold change was then calculated by comparison of signal intensities. Fold changes greater or less than 2-fold were subject gene ontology analysis(Ingenuity Systems) with a statistical threshold of p=0.01.

ChIP assay. Snap frozen TA muscle from WT and Sox6 cKO mice was minced on ice and fixed with 4% PFA at room temperature for 15 minutes. Samples were quenched, washed, and dounce homogenized in lysis buffer(EZ ChIP kit, Millipore). Samples were sonicated using a bioruptor (Diagenode) and further prepared using EZ-ChIP kit(Millipore) according to manufacturers instructions. Antibody directed against the N-terminus of Sox6(Han and Lefebvre, 2008) was kindly provided by Dr. Veronique Lefebvre. C2C12 myoblasts were transfected

with n-terminal tagged FLAG-Sox6. C2C12 ChIP was performed using EZ-ChIP kit and anti-FLAG antibody(Sigma).

Western Blotting. Protein was isolated from muscle by dounce homogenization in RIPA buffer containing protease inhibitor cocktail(Roche). Protein concentrations were determined by BCA Protein assay(Thermo Scientific) and samples were resolved by SDS-PAGE electrophoresis. Tnni1 and myoglobin were detected by anti-Tnni1 primary antibody(sc-8119) at a concentration of 1:1000, and α-myoglobin primary antibody(Dako) at a concentration of 1:5000. Appropriate HRP-conjugated secondary antibodies(Biorad) at a concentration of 1:5000 and chemiluminescent reagent(Santa Cruz) were used for detection.

ChIP Primers:

myl3-F	GAGGCCTCTGTCTCCCTCTC
myl3-R	CTGCTCAAGGGGCTATTTTG
myl2-F	CTCCGCCTCACCTACAACTG
myl2-R	ACCTCTGGAGAGTTCGAGGA
myh7-F	TAAAAGCATTTCCCCCGACT
myh7-R	CCTGGAACTCAGACCCTGAA
myh1-F	GGGCTCAGTCTCAGTCATGC
myh1-R	CAGCAGCCTCGGTGGTAT
ATP2a2-F	CTAGATTGTGAAGTGCCATTGAA
ATP2a2-R	GACTGGGTTTCTGTCCCTTC

Gel Shift Oligos:

myh7-F	GCTAGGAAACAATTGGAAGTGGTCGTCATTGTTGTGGCA
myh7-R	TGCCACAACAATGACGACCACTTCCAATTGTTTCCTAGC
myl3-F	CCATTCCTGGGCTTGAACAATGCCCTCTCCAGGA

myl3-R	TCCTGGAGAGGGCATTGTTCAAGCCCAGGAATGG
myl2-F	GAGAGGTATTTATTGTTCCACAGCAGGGGCAG
myl2-R	CTGCCCCTGCTGTGGAACAATAAATACCTCTC
myh1-F	TTAAAATAGGAAACAATGTTCAGGTGTTATT
myh1-R	AATAACACCTGAACATTGTTTCCTATTTTAA
ATP2a2-F	AATGTTGGCAAAACAATGTCTGTTACAATA
ATP2a2-R	TATTGTAACAGACATTGTTTTGCCAACATT
myh7-MUT-F	GCTAGGAGAGACGTGGAAGTGGTCGTCCGTCTCGTGGCA
myh7-MUT-R	TGCCACGAGACGGACGACCACTTCCACGTCTCTCCTAGC
myh1-MUT-F	TTAAAATAGGAGAGACGGTTCAGGTGTTATT
myh1-MUT-R	AATAACACCTGAACCGTCTCTCCTATTTTAA
myl2-MUT-F	GAGAGGTATTTCGTCTCCCACAGCAGGGGCAG
myl2-MUT-R	CTGCCCCTGCTGTGGGAGACGAAATACCTCTC
myl3-MUT-F	CCATTCCTGGGCTTGGAGACGGCCCTCTCCAGGA
myl3-MUT-R	TCCTGGAGAGGGCCGTCTCCAAGCCCAGGAATGG
ATP2a2-MUT-F	AATGTTGGCAAGAGACGGTCTGTTACAATA
ATP2a2-MUT-R	TATTGTAACAGACCGTCTCTTGCCAACATT

Sybr Green Primers:

sv2b-SYBR-F	TTCCCAGTTTATCAGCCAGG
sv2b-SYBR-R	TAGTGAGCTTTGCTCTGCCA
cryba4-SYBR-F	GCCCCTCTCCAGCACATATT
cryba4-SYBR-R	TCACAGCTGAGTGTCCCAGT
chrna1-SYBR-F	ACAATCTCACGGTGGTCCTC
chrna1-SYBR-R	CTGTTCTCCTGCTGCTAGGC
Psat1-SYBR-F	CATTTGGGATTTGATGGAGC
Psat1-SYBR-R	ACTACAAAGTGCAGGCTGGG
crybb1-SYBR-F	GGAAGGCAGATTGCTCAAAG
crybb1-SYBR-R	GATCGTCTTCGAGCAGGAAA
Vlrd6-SYBR-F	GGCGCCTTCAGGATCATA
Vlrd6-SYBR-R	TCATGGCTCAGCACTCATCT
Lrba-SYBR-F	GCCTCAAGTCATCTTCCCAG
Lrba-SYBR-R	GAGACCATGTGACCGCAAC
Sln-SYBR-F	CACACCAAGGCTTGTCTTCA
Sln-SYBR-R	CCCTCAGACTACATTAGGCCC
Pdrg1-SYBR-F	AAAACCTTTCAGCTCCGGTT
Pdrg1-SYBR-R	ATGCCTCACCCTAAGACGAA
Mod1-SYBR-F	ATGCCATATTTGGAAGACGC
Mod1-SYBR-R	TCACTTTGGATGTGGGAACA
Psdm8-SYBR-F	TGTGTGGAACTCAGCCACTC
Psdm8-SYBR-R	TACATGGCCCAACTCAAATG
Rpl29-SYBR-F	TCTTGTTGTGCTTCTTGGCA

Rpl29-SYBR-R	GAACCACACCACACACAACC
Lrrc2-SYBR-F	AGGTGATCCCCACTGACAAC
Lrrc2-SYBR-R	CTGAGTGACCTGCCACAAGA
Smox-SYBR-F	CGCCACTGGATTCACAACTT
Smox-SYBR-R	TGCAGGAGGAAGCCCAGT
kcnc4-SYBR-F	CTACCCGATGAATCTCCGTC
kcnc4-SYBR-R	GAGGATCCCTACTCATCCCG
opn1mw-SYBR-F	GTCTTGGAGGTGCTGGAAAG
opn1mw-SYBR-R	GGCCTCCCTACCATCCTACT
LOC225594-SYBR-F	ATGTGAAGAGCCTGGAGCAC
LOC225594-SYBR-R	CAGTGAAGCTGGACTCCAAA
dysfip1-SYBR-F	CTTGGACCACATTCGACAAG
dysfip1-SYBR-R	ATGTCAGCCCCGTATTTGAC
LOC383308-SYBR-F	CACGAAACACACCACACACA
LOC383308-SYBR-R	TTCAGGGCTTTCTTGTGCTT
zymnd17-SYBR-F	GTCATGGAATGGCTTCTGGT
zymnd17-SYBR-R	GCCCAAAGCATGGTCATAGA
KLK26-F1-sybr	CCCCACAAATGTGTTCCTTT
KLK26-R1-sybr	GTTCCTGATCCTGTTCCCAG
KLK22-F1-sybr	GACTCCCCCGCATAGGTACT
KLK22-R1-sybr	CCTGTTCCTAACCCTGTCCC
LRRN1-F1-sybr	CACAGGTCCTTGTGGGAGTT
LRRN1-R1-sybr	TCCTCATCCTCCGGCTAGT
DUPD1-F1-sybr	GCCGGACTACTACCGAGACA
DUPD1-R1-sybr	GCGGTTCTTAGCCACTTGTT
RSPO3-F1-sybr	ATCTGAACACGTTGCACAGC
RSPO3-R1-sybr	CTTTATGGAATACATTGGCAGC

CHAPTER V

Conclusion and Further Remarks

In this study, we established that two myosin encoded microRNAs are necessary and sufficient to promote the differentiation of slow myofibers *in vivo*. Furthermore, we show that the direct downstream target gene Sox6 directly represses the expression of multiple genes that encode components of the sarcomere in slow myofibers. Thus, the MyomiRs serve as a nexus between slow myofiber stimuli, such as calcineurin activation by increased intracellular calcium or the hypothyroid state, to dampen Sox6 activity and promote a slow myofiber phenotype (Figure 5.1).

Intriguingly, it appears that the *in vivo* genetic studies of the MyomiR target Sox6 recapitulate the phenotype observed in the gain and loss-of-function studies of miR-208b/499. Most microRNAs are hypothesized to act through their repression of a multitude of mRNA targets, however, in this case it seems that Sox6 might be the primary target that mediates the effects of MyomiRs on myofiber phenotype. Direct comparison of the transcriptomes of MCK-miR-499 transgenic and Sox6 cKO skeletal muscle by RNA-Seq could potentially

implicate Sox6 as the primary downstream effector of the MyomiRs, or identify other MyomiR targets that influence muscle fiber type contraction or metabolism.

Given the importance of Sox6 as a MyomiR target in skeletal muscle, further studies are needed to elucidate the role of Sox6 in cardiac muscle. Work in mice carrying an inversion allele that globally disrupts Sox6 expression suggests that Sox6 plays a role in cardiomyocyte development and cardiac conduction (Cohen-Barak et al., 2003). In order to overcome the lethality associated with global deletion of Sox6, studies utilizing cardiac specific ablation of Sox6 expression in the embryo and adult will be informative of its role in cardiac function.

Genetic studies in mice have shown that an increase in slow muscle fibers confers resistance to musculoskeletal and metabolic disease. In the future, we plan to study the effects of the MyomiR regulatory network on the pathogenesis of type II diabetes induced hyperglycemia and obesity. Perhaps miR-208b/499 mimic oligonucleotides, or identification and pharmacological inhibition of Sox6 and its binding partners in skeletal muscle could confer a therapeutic shift in skeletal muscle fiber type. Small molecule inhibitors of the SOX6-BCL11A complex have been shown to therapeutically alter hemoglobin expression and to be efficacious in the treatment of models of sickle cell anemia (Xu et al., 2011).

Our results suggest a significant role for the MyomiR-Sox6 regulatory axis in the complex phenotypic remodeling of muscle fiber type. This work has

identified a biologically important feed-forward signaling cascade in skeletal muscle, and in our future studies of this pathway we aim to further identify molecular mechanisms underlying fiber type transitions, decode the function of novel myofiber enriched genes, and understanding the connection between muscle fiber type and whole body metabolism.

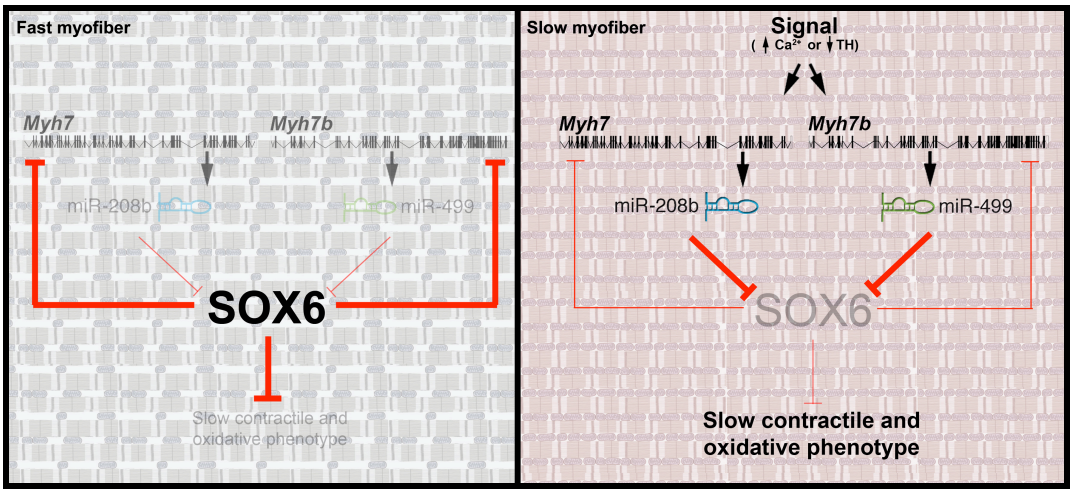

Figure 5.1 Model of the MyomiR regulatory network in skeletal muscle.

References

Adolph, E.A., Subramaniam, A., Cserjesi, P., Olson, E.N., and Robbins, J. (1993). Role of myocyte-specific enhancer-binding factor (MEF-2) in transcriptional regulation of the alpha-cardiac myosin heavy chain gene. J Biol Chem *268*, 5349-5352.

Allen, D.L., Harrison, B.C., Maass, A., Bell, M.L., Byrnes, W.C., and Leinwand, L.A. (2001). Cardiac and skeletal muscle adaptations to voluntary wheel running in the mouse. J Appl Physiol *90*, 1900-1908.

An, C.I., Dong, Y., and Hagiwara, N. (2011). Genome-wide mapping of Sox6 binding sites in skeletal muscle reveals both direct and indirect regulation of muscle terminal differentiation by Sox6. BMC Dev Biol *11*, 59.

Arany, Z., Lebrasseur, N., Morris, C., Smith, E., Yang, W., Ma, Y., Chin, S., and Spiegelman, B.M. (2007). The transcriptional coactivator PGC-1beta drives the formation of oxidative type IIX fibers in skeletal muscle. Cell Metab *5*, 35-46.

Azakie, A., Fineman, J.R., and He, Y. (2006). Sp3 inhibits Sp1-mediated activation of the cardiac troponin T promoter and is downregulated during pathological cardiac hypertrophy in vivo. Am J Physiol Heart Circ Physiol *291*, H600-611.

Baek, D., Villen, J., Shin, C., Camargo, F.D., Gygi, S.P., and Bartel, D.P. (2008). The impact of microRNAs on protein output. Nature *455*, 64-71.

Baldwin, K.M., and Haddad, F. (2001). Effects of different activity and inactivity paradigms on myosin heavy chain gene expression in striated muscle. J Appl Physiol *90*, 345-357.

Bandman, E. (1992). Contractile protein isoforms in muscle development. Dev Biol *154*, 273-283.

Bartel, D.P. (2004). MicroRNAs: genomics, biogenesis, mechanism, and function. Cell *116*, 281-297.

Bassel-Duby, R., and Olson, E.N. (2006). Signaling pathways in skeletal muscle remodeling. Annu Rev Biochem *75*, 19-37.

Biering-Sorensen, B., Kristensen, I.B., Kjaer, M., and Biering-Sorensen, F. (2009). Muscle after spinal cord injury. Muscle Nerve *40*, 499-519.

Bottinelli, R., Schiaffino, S., and Reggiani, C. (1991). Force-velocity relations and myosin heavy chain isoform compositions of skinned fibres from rat skeletal muscle. J Physiol *437*, 655-672.

Bowles, J., Schepers, G., and Koopman, P. (2000). Phylogeny of the SOX family of developmental transcription factors based on sequence and structural indicators. Dev Biol *227*, 239-255.

Brooks, S.V., and Faulkner, J.A. (1988). Contractile properties of skeletal muscles from young, adult and aged mice. The Journal of physiology *404*, 71-82.

Brooks, S.V., Faulkner, J.A., and McCubbrey, D.A. (1990). Power outputs of slow and fast skeletal muscles of mice. J Appl Physiol *68*, 1282-1285.

Bruce Alberts, A.J., Julian Lewis, Martin Raff, Keith Roberts, and Peter Walter (2002). Molecular Biology of the Cell, 4th edition (New York, Garland Science).

Bruning, J.C., Michael, M.D., Winnay, J.N., Hayashi, T., Horsch, D., Accili, D., Goodyear, L.J., and Kahn, C.R. (1998). A muscle-specific insulin receptor knockout exhibits features of the metabolic syndrome of NIDDM without altering glucose tolerance. Mol Cell *2*, 559-569.

Buchthal, F., and Schmalbruch, H. (1980). Motor unit of mammalian muscle. Physiol Rev *60*, 90-142.

Call, J.A., Voelker, K.A., Wolff, A.V., McMillan, R.P., Evans, N.P., Hulver, M.W., Talmadge, R.J., and Grange, R.W. (2008). Endurance capacity in maturing

mdx mice is markedly enhanced by combined voluntary wheel running and green tea extract. J Appl Physiol *105*, 923-932.

Callis, T.E., Pandya, K., Seok, H.Y., Tang, R.H., Tatsuguchi, M., Huang, Z.P., Chen, J.F., Deng, Z., Gunn, B., Shumate, J.*, et al.* (2009). MicroRNA-208a is a regulator of cardiac hypertrophy and conduction in mice. J Clin Invest *119*, 2772-2786.

Calvo, S., Venepally, P., Cheng, J., and Buonanno, A. (1999). Fiber-type-specific transcription of the troponin I slow gene is regulated by multiple elements. Mol Cell Biol *19*, 515-525.

Chen, J.F., Mandel, E.M., Thomson, J.M., Wu, Q., Callis, T.E., Hammond, S.M., Conlon, F.L., and Wang, D.Z. (2006). The role of microRNA-1 and microRNA-133 in skeletal muscle proliferation and differentiation. Nat Genet *38*, 228-233.

Chin, E.R., Olson, E.N., Richardson, J.A., Yang, Q., Humphries, C., Shelton, J.M., Wu, H., Zhu, W., Bassel-Duby, R., and Williams, R.S. (1998). A calcineurin-dependent transcriptional pathway controls skeletal muscle fiber type. Genes Dev *12*, 2499-2509.

Choi, C.S., Befroy, D.E., Codella, R., Kim, S., Reznick, R.M., Hwang, Y.J., Liu, Z.X., Lee, H.Y., Distefano, A., Samuel, V.T.*, et al.* (2008). Paradoxical effects of increased expression of PGC-1alpha on muscle mitochondrial function and

insulin-stimulated muscle glucose metabolism. Proc Natl Acad Sci U S A *105*, 19926-19931.

Claverie, J.M. (2001). Gene number. What if there are only 30,000 human genes? Science *291*, 1255-1257.

Cohen-Barak, O., Yi, Z., Hagiwara, N., Monzen, K., Komuro, I., and Brilliant, M.H. (2003). Sox6 regulation of cardiac myocyte development. Nucleic Acids Res *31*, 5941-5948.

Connor, F., Wright, E., Denny, P., Koopman, P., and Ashworth, A. (1995). The Sry-related HMG box-containing gene Sox6 is expressed in the adult testis and developing nervous system of the mouse. Nucleic Acids Res *23*, 3365-3372.

Crabtree, G.R., and Olson, E.N. (2002). NFAT signaling: choreographing the social lives of cells. Cell *109 Suppl*, S67-79.

Dumitriu, B., Dy, P., Smits, P., and Lefebvre, V. (2006). Generation of mice harboring a Sox6 conditional null allele. Genesis *44*, 219-224.

Eisenberg, I., Eran, A., Nishino, I., Moggio, M., Lamperti, C., Amato, A.A., Lidov, H.G., Kang, P.B., North, K.N., Mitrani-Rosenbaum, S.*, et al.* (2007). Distinctive patterns of microRNA expression in primary muscular disorders. Proc Natl Acad Sci U S A *104*, 17016-17021.

Fickett, J.W., and Wasserman, W.W. (2000). Discovery and modeling of transcriptional regulatory regions. Curr Opin Biotechnol *11*, 19-24.

Fiori, M.G., Andreola, S., Ladelli, G., and Scirea, M.R. (1983). Selective atrophy of the type IIb muscle fibers in rheumatoid arthritis and progressive systemic sclerosis (scleroderma). A biopsy histochemical study. Eur J Rheumatol Inflamm *6*, 168-181.

Gan, Z., Burkart-Hartman, E.M., Han, D.H., Finck, B., Leone, T.C., Smith, E.Y., Ayala, J.E., Holloszy, J., and Kelly, D.P. (2011). The nuclear receptor PPARbeta/delta programs muscle glucose metabolism in cooperation with AMPK and MEF2. Genes Dev *25*, 2619-2630.

Geiger, P.C., Cody, M.J., and Sieck, G.C. (1999). Force-calcium relationship depends on myosin heavy chain and troponin isoforms in rat diaphragm muscle fibers. J Appl Physiol *87*, 1894-1900.

Grange, R.W., Cory, C.R., Vandenboom, R., and Houston, M.E. (1995). Myosin phosphorylation augments force-displacement and force-velocity relationships of mouse fast muscle. The American journal of physiology *269*, C713-724.

Grange, R.W., Gainer, T.G., Marschner, K.M., Talmadge, R.J., and Stull, J.T. (2002). Fast-twitch skeletal muscles of dystrophic mouse pups are resistant to

injury from acute mechanical stress. American journal of physiology *283*, C1090-1101.

Grifone, R., Laclef, C., Spitz, F., Lopez, S., Demignon, J., Guidotti, J.E., Kawakami, K., Xu, P.X., Kelly, R., Petrof, B.J.*, et al.* (2004). Six1 and Eya1 expression can reprogram adult muscle from the slow-twitch phenotype into the fast-twitch phenotype. Mol Cell Biol *24*, 6253-6267.

Guo, H., Ingolia, N.T., Weissman, J.S., and Bartel, D.P. (2010). Mammalian microRNAs predominantly act to decrease target mRNA levels. Nature *466*, 835-840.

Gupta, M., Sueblinvong, V., Raman, J., Jeevanandam, V., and Gupta, M.P. (2003). Single-stranded DNA-binding proteins PURalpha and PURbeta bind to a purine-rich negative regulatory element of the alpha-myosin heavy chain gene and control transcriptional and translational regulation of the gene expression. Implications in the repression of alpha-myosin heavy chain during heart failure. J Biol Chem *278*, 44935-44948.

Hagiwara, N., Ma, B., and Ly, A. (2005). Slow and fast fiber isoform gene expression is systematically altered in skeletal muscle of the Sox6 mutant, p100H. Dev Dyn *234*, 301-311.

Hagiwara, N., Yeh, M., and Liu, A. (2007). Sox6 is required for normal fiber type differentiation of fetal skeletal muscle in mice. Dev Dyn *236*, 2062-2076.

Halseth, A.E., Bracy, D.P., and Wasserman, D.H. (2001). Functional limitations to glucose uptake in muscles comprised of different fiber types. Am J Physiol Endocrinol Metab *280*, E994-999.

Han, Y., and Lefebvre, V. (2008). L-Sox5 and Sox6 drive expression of the aggrecan gene in cartilage by securing binding of Sox9 to a far-upstream enhancer. Mol Cell Biol *28*, 4999-5013.

Harvey Lodish, A.B., S Lawrence Zipursky, Paul Matsudaira, David Baltimore, and James Darnell (2000). Molecular Cell Biology, 4th edition, 4th edn (New York, W. H. Freeman).

Holloszy, J.O., and Booth, F.W. (1976). Biochemical adaptations to endurance exercise in muscle. Annu Rev Physiol *38*, 273-291.

Ikeda, T., Zhang, J., Chano, T., Mabuchi, A., Fukuda, A., Kawaguchi, H., Nakamura, K., and Ikegawa, S. (2002). Identification and characterization of the human long form of Sox5 (L-SOX5) gene. Gene *298*, 59-68.

Izumiya, Y., Hopkins, T., Morris, C., Sato, K., Zeng, L., Viereck, J., Hamilton, J.A., Ouchi, N., LeBrasseur, N.K., and Walsh, K. (2008). Fast/Glycolytic muscle

fiber growth reduces fat mass and improves metabolic parameters in obese mice. Cell Metab *7*, 159-172.

Ji, J., Tsika, G.L., Rindt, H., Schreiber, K.L., McCarthy, J.J., Kelm, R.J., Jr., and Tsika, R. (2007). Puralpha and Purbeta collaborate with Sp3 to negatively regulate beta-myosin heavy chain gene expression during skeletal muscle inactivity. Mol Cell Biol *27*, 1531-1543.

Karpati, G., and Engel, W.K. (1968). "Type grouping" in skeletal muscles after experimental reinnervation. Neurology *18*, 447-455.

Kim, H.K., Lee, Y.S., Sivaprasad, U., Malhotra, A., and Dutta, A. (2006). Muscle-specific microRNA miR-206 promotes muscle differentiation. J Cell Biol *174*, 677-687.

Larsson, L., Muller, U., Li, X., and Schiaffino, S. (1995). Thyroid hormone regulation of myosin heavy chain isoform composition in young and old rats, with special reference to IIX myosin. Acta Physiol Scand *153*, 109-116.

Lefebvre, V. (2002). Toward understanding the functions of the two highly related Sox5 and Sox6 genes. J Bone Miner Metab *20*, 121-130.

Lefebvre, V., Li, P., and de Crombrugghe, B. (1998). A new long form of Sox5 (L-Sox5), Sox6 and Sox9 are coexpressed in chondrogenesis and cooperatively activate the type II collagen gene. EMBO J *17*, 5718-5733.

Lehman, W., Craig, R., and Vibert, P. (1994). Ca(2+)-induced tropomyosin movement in Limulus thin filaments revealed by three-dimensional reconstruction. Nature *368*, 65-67.

Lexell, J. (1995). Human aging, muscle mass, and fiber type composition. J Gerontol A Biol Sci Med Sci *50 Spec No*, 11-16.

Lillioja, S., Young, A.A., Culter, C.L., Ivy, J.L., Abbott, W.G., Zawadzki, J.K., Yki-Jarvinen, H., Christin, L., Secomb, T.W., and Bogardus, C. (1987). Skeletal muscle capillary density and fiber type are possible determinants of in vivo insulin resistance in man. J Clin Invest *80*, 415-424.

Lin, J., Wu, H., Tarr, P.T., Zhang, C.Y., Wu, Z., Boss, O., Michael, L.F., Puigserver, P., Isotani, E., Olson, E.N.*, et al.* (2002). Transcriptional co-activator PGC-1 alpha drives the formation of slow-twitch muscle fibres. Nature *418*, 797-801.

Linssen, W.H., Stegeman, D.F., Joosten, E.M., Binkhorst, R.A., Merks, M.J., ter Laak, H.J., and Notermans, S.L. (1991). Fatigue in type I fiber predominance: a

muscle force and surface EMG study on the relative role of type I and type II muscle fibers. Muscle Nerve *14*, 829-837.

Liu, N., Bezprozvannaya, S., Shelton, J.M., Frisard, M.I., Hulver, M.W., McMillan, R.P., Wu, Y., Voelker, K.A., Grange, R.W., Richardson, J.A.*, et al.* (2011). Mice lacking microRNA 133a develop dynamin 2-dependent centronuclear myopathy. J Clin Invest *121*, 3258-3268.

Liu, N., Bezprozvannaya, S., Williams, A.H., Qi, X., Richardson, J.A., Bassel-Duby, R., and Olson, E.N. (2008). microRNA-133a regulates cardiomyocyte proliferation and suppresses smooth muscle gene expression in the heart. Genes Dev *22*, 3242-3254.

Liu, N., Williams, A.H., Kim, Y., McAnally, J., Bezprozvannaya, S., Sutherland, L.B., Richardson, J.A., Bassel-Duby, R., and Olson, E.N. (2007). An intragenic MEF2-dependent enhancer directs muscle-specific expression of microRNAs 1 and 133. Proc Natl Acad Sci U S A *104*, 20844-20849.

Lompre, A.M., Nadal-Ginard, B., and Mahdavi, V. (1984). Expression of the cardiac ventricular alpha- and beta-myosin heavy chain genes is developmentally and hormonally regulated. J Biol Chem *259*, 6437-6446.

Martindale, M.Q. (2005). The evolution of metazoan axial properties. Nat Rev Genet *6*, 917-927.

McAllister, R.M., Ogilvie, R.W., and Terjung, R.L. (1991). Functional and metabolic consequences of skeletal muscle remodeling in hypothyroidism. Am J Physiol *260*, E272-279.

McCall, G.E., Byrnes, W.C., Dickinson, A., Pattany, P.M., and Fleck, S.J. (1996). Muscle fiber hypertrophy, hyperplasia, and capillary density in college men after resistance training. J Appl Physiol *81*, 2004-2012.

McGuigan, K., Phillips, P.C., and Postlethwait, J.H. (2004). Evolution of sarcomeric myosin heavy chain genes: evidence from fish. Mol Biol Evol *21*, 1042-1056.

McKinsey, T.A., Zhang, C.L., and Olson, E.N. (2001). Control of muscle development by dueling HATs and HDACs. Curr Opin Genet Dev *11*, 497-504.

Mercer, T.R., Dinger, M.E., and Mattick, J.S. (2009). Long non-coding RNAs: insights into functions. Nat Rev Genet *10*, 155-159.

Moss, E.G., Lee, R.C., and Ambros, V. (1997). The cold shock domain protein LIN-28 controls developmental timing in C. elegans and is regulated by the lin-4 RNA. Cell *88*, 637-646.

Nadal-Ginard, B., and Mahdavi, V. (1989). Molecular basis of cardiac performance. Plasticity of the myocardium generated through protein isoform switches. J Clin Invest *84*, 1693-1700.

Najafi-Shoushtari, S.H., Kristo, F., Li, Y., Shioda, T., Cohen, D.E., Gerszten, R.E., and Naar, A.M. (2010). MicroRNA-33 and the SREBP host genes cooperate to control cholesterol homeostasis. Science *328*, 1566-1569.

Narkar, V.A., Downes, M., Yu, R.T., Embler, E., Wang, Y.X., Banayo, E., Mihaylova, M.M., Nelson, M.C., Zou, Y., Juguilon, H.*, et al.* (2008). AMPK and PPARdelta agonists are exercise mimetics. Cell *134*, 405-415.

Naya, F.J., Mercer, B., Shelton, J., Richardson, J.A., Williams, R.S., and Olson, E.N. (2000). Stimulation of slow skeletal muscle fiber gene expression by calcineurin in vivo. J Biol Chem *275*, 4545-4548.

Nielsen, M., Hansen, J.H., Hedegaard, J., Nielsen, R.O., Panitz, F., Bendixen, C., and Thomsen, B. (2010). MicroRNA identity and abundance in porcine skeletal muscles determined by deep sequencing. Anim Genet *41*, 159-168.

O'Rourke, J.R., Georges, S.A., Seay, H.R., Tapscott, S.J., McManus, M.T., Goldhamer, D.J., Swanson, M.S., and Harfe, B.D. (2007). Essential role for Dicer during skeletal muscle development. Dev Biol *311*, 359-368.

Ogilvie, R.W., and Feeback, D.L. (1990). A metachromatic dye-ATPase method for the simultaneous identification of skeletal muscle fiber types I, IIA, IIB and IIC. Stain Technol *65*, 231-241.

Parrizas, M., Maestro, M.A., Banos, N., Navarro, I., Planas, J., and Gutierrez, J. (1995). Insulin/IGF-I binding ratio in skeletal and cardiac muscles of vertebrates: a phylogenetic approach. Am J Physiol *269*, R1370-1377.

Pauli, A., Rinn, J.L., and Schier, A.F. (2011). Non-coding RNAs as regulators of embryogenesis. Nat Rev Genet *12*, 136-149.

Pette, D., and Staron, R.S. (1997). Mammalian skeletal muscle fiber type transitions. Int Rev Cytol *170*, 143-223.

Pette, D., and Staron, R.S. (2000). Myosin isoforms, muscle fiber types, and transitions. Microsc Res Tech *50*, 500-509.

Potthoff, M.J., and Olson, E.N. (2007). MEF2: a central regulator of diverse developmental programs. Development *134*, 4131-4140.

Potthoff, M.J., Wu, H., Arnold, M.A., Shelton, J.M., Backs, J., McAnally, J., Richardson, J.A., Bassel-Duby, R., and Olson, E.N. (2007). Histone deacetylase degradation and MEF2 activation promote the formation of slow-twitch myofibers. J Clin Invest *117*, 2459-2467.

Ranvier, L. (1873). Proprietés et structures différentes des muscles rouges et des muscles blancs chez les
lapins et chez les raies. C r Acad Sci Paris, 1030–1034.

Rao, P.K., Kumar, R.M., Farkhondeh, M., Baskerville, S., and Lodish, H.F. (2006). Myogenic factors that regulate expression of muscle-specific microRNAs. Proc Natl Acad Sci U S A *103*, 8721-8726.

Reinhart, B.J., Slack, F.J., Basson, M., Pasquinelli, A.E., Bettinger, J.C., Rougvie, A.E., Horvitz, H.R., and Ruvkun, G. (2000). The 21-nucleotide let-7 RNA regulates developmental timing in Caenorhabditis elegans. Nature *403*, 901-906.

Rockl, K.S., Hirshman, M.F., Brandauer, J., Fujii, N., Witters, L.A., and Goodyear, L.J. (2007). Skeletal muscle adaptation to exercise training: AMP-activated protein kinase mediates muscle fiber type shift. Diabetes *56*, 2062-2069.

Salmena, L., Poliseno, L., Tay, Y., Kats, L., and Pandolfi, P.P. (2011). A ceRNA hypothesis: the Rosetta Stone of a hidden RNA language? Cell *146*, 353-358.

Sandri, M., Lin, J., Handschin, C., Yang, W., Arany, Z.P., Lecker, S.H., Goldberg, A.L., and Spiegelman, B.M. (2006). PGC-1alpha protects skeletal muscle from atrophy by suppressing FoxO3 action and atrophy-specific gene transcription. Proc Natl Acad Sci U S A *103*, 16260-16265.

Sato, I., Wu, S., Ibarra, M.C., Hayashi, Y.K., Fujita, H., Tojo, M., Oh, S.J., Nonaka, I., Noguchi, S., and Nishino, I. (2008). Congenital neuromuscular disease with uniform type 1 fiber and RYR1 mutation. Neurology *70*, 114-122.

Schiaffino, S. (2011). Fibre types in skeletal muscle: a personal account. Acta Physiol (Oxf) *199*, 451-463.

Schuler, M., Ali, F., Chambon, C., Duteil, D., Bornert, J.M., Tardivel, A., Desvergne, B., Wahli, W., Chambon, P., and Metzger, D. (2006). PGC1alpha expression is controlled in skeletal muscles by PPARbeta, whose ablation results in fiber-type switching, obesity, and type 2 diabetes. Cell Metab *4*, 407-414.

Seipel, K., and Schmid, V. (2005). Evolution of striated muscle: jellyfish and the origin of triploblasty. Dev Biol *282*, 14-26.

Shulman, A.I., and Mangelsdorf, D.J. (2005). Retinoid x receptor heterodimers in the metabolic syndrome. N Engl J Med *353*, 604-615.

Smits, P., Li, P., Mandel, J., Zhang, Z., Deng, J.M., Behringer, R.R., de Crombrugghe, B., and Lefebvre, V. (2001). The transcription factors L-Sox5 and Sox6 are essential for cartilage formation. Dev Cell *1*, 277-290.

Spudich, J.A. (2001). The myosin swinging cross-bridge model. Nat Rev Mol Cell Biol *2*, 387-392.

Staron, R.S., Gohlsch, B., and Pette, D. (1987). Myosin polymorphism in single fibers of chronically stimulated rabbit fast-twitch muscle. Pflugers Arch *408*, 444-450.

Sternberg, E.A., Spizz, G., Perry, W.M., Vizard, D., Weil, T., and Olson, E.N. (1988). Identification of upstream and intragenic regulatory elements that confer cell-type-restricted and differentiation-specific expression on the muscle creatine kinase gene. Mol Cell Biol *8*, 2896-2909.

Stolt, C.C., Schlierf, A., Lommes, P., Hillgartner, S., Werner, T., Kosian, T., Sock, E., Kessaris, N., Richardson, W.D., Lefebvre, V.*, et al.* (2006). SoxD proteins influence multiple stages of oligodendrocyte development and modulate SoxE protein function. Dev Cell *11*, 697-709.

Struhl, K. (1999). Fundamentally different logic of gene regulation in eukaryotes and prokaryotes. Cell *98*, 1-4.

Talmadge, R.J., and Roy, R.R. (1993). Electrophoretic separation of rat skeletal muscle myosin heavy-chain isoforms. J Appl Physiol *75*, 2337-2340.

Tanner, C.J., Barakat, H.A., Dohm, G.L., Pories, W.J., MacDonald, K.G., Cunningham, P.R., Swanson, M.S., and Houmard, J.A. (2002). Muscle fiber type is associated with obesity and weight loss. Am J Physiol Endocrinol Metab *282*, E1191-1196.

Templeton, G.H., Sweeney, H.L., Timson, B.F., Padalino, M., and Dudenhoeffer, G.A. (1988). Changes in fiber composition of soleus muscle during rat hindlimb suspension. J Appl Physiol *65*, 1191-1195.

Tsika, G., Ji, J., and Tsika, R. (2004). Sp3 proteins negatively regulate beta myosin heavy chain gene expression during skeletal muscle inactivity. Mol Cell Biol *24*, 10777-10791.

van Rooij, E., Liu, N., and Olson, E.N. (2008). MicroRNAs flex their muscles. Trends Genet *24*, 159-166.

van Rooij, E., Quiat, D., Johnson, B.A., Sutherland, L.B., Qi, X., Richardson, J.A., Kelm, R.J., Jr., and Olson, E.N. (2009). A family of microRNAs encoded by myosin genes governs myosin expression and muscle performance. Dev Cell *17*, 662-673.

van Rooij, E., Sutherland, L.B., Liu, N., Williams, A.H., McAnally, J., Gerard, R.D., Richardson, J.A., and Olson, E.N. (2006). A signature pattern of stress-responsive microRNAs that can evoke cardiac hypertrophy and heart failure. Proc Natl Acad Sci U S A *103*, 18255-18260.

van Rooij, E., Sutherland, L.B., Qi, X., Richardson, J.A., Hill, J., and Olson, E.N. (2007). Control of stress-dependent cardiac growth and gene expression by a microRNA. Science *316*, 575-579.

von Hofsten, J., Elworthy, S., Gilchrist, M.J., Smith, J.C., Wardle, F.C., and Ingham, P.W. (2008). Prdm1- and Sox6-mediated transcriptional repression specifies muscle fibre type in the zebrafish embryo. EMBO Rep *9*, 683-689.

Wang, Y.X., Zhang, C.L., Yu, R.T., Cho, H.K., Nelson, M.C., Bayuga-Ocampo, C.R., Ham, J., Kang, H., and Evans, R.M. (2004). Regulation of muscle fiber type and running endurance by PPARdelta. PLoS Biol *2*, e294.

Wiersma, C.A. (1952). Comparative physiology of invertebrate muscle. Annu Rev Physiol *14*, 159-176.

Williams, A.H., Valdez, G., Moresi, V., Qi, X., McAnally, J., Elliott, J.L., Bassel-Duby, R., Sanes, J.R., and Olson, E.N. (2009). MicroRNA-206 delays ALS progression and promotes regeneration of neuromuscular synapses in mice. Science *326*, 1549-1554.

Wolff, A.V., Niday, A.K., Voelker, K.A., Call, J.A., Evans, N.P., Granata, K.P., and Grange, R.W. (2006). Passive mechanical properties of maturing extensor digitorum longus are not affected by lack of dystrophin. Muscle & nerve *34*, 304-312.

Wright, C.E., Haddad, F., Qin, A.X., Bodell, P.W., and Baldwin, K.M. (1999). In vivo regulation of beta-MHC gene in rodent heart: role of T3 and evidence for an upstream enhancer. Am J Physiol *276*, C883-891.

Wu, H., Naya, F.J., McKinsey, T.A., Mercer, B., Shelton, J.M., Chin, E.R., Simard, A.R., Michel, R.N., Bassel-Duby, R., Olson, E.N., *et al.* (2000). MEF2 responds to multiple calcium-regulated signals in the control of skeletal muscle fiber type. EMBO J *19*, 1963-1973.

Wu, H., Rothermel, B., Kanatous, S., Rosenberg, P., Naya, F.J., Shelton, J.M., Hutcheson, K.A., DiMaio, J.M., Olson, E.N., Bassel-Duby, R., *et al.* (2001). Activation of MEF2 by muscle activity is mediated through a calcineurin-dependent pathway. EMBO J *20*, 6414-6423.

Wu, Z., Puigserver, P., Andersson, U., Zhang, C., Adelmant, G., Mootha, V., Troy, A., Cinti, S., Lowell, B., Scarpulla, R.C., *et al.* (1999). Mechanisms controlling mitochondrial biogenesis and respiration through the thermogenic coactivator PGC-1. Cell *98*, 115-124.

Xu, J., Peng, C., Sankaran, V.G., Shao, Z., Esrick, E.B., Chong, B.G., Ippolito, G.C., Fujiwara, Y., Ebert, B.L., Tucker, P.W., *et al.* (2011). Correction of sickle cell disease in adult mice by interference with fetal hemoglobin silencing. Science *334*, 993-996.

Xu, J., Sankaran, V.G., Ni, M., Menne, T.F., Puram, R.V., Kim, W., and Orkin, S.H. (2010). Transcriptional silencing of {gamma}-globin by BCL11A involves long-range interactions and cooperation with SOX6. Genes Dev *24*, 783-798.

Yu, F., Gothe, S., Wikstrom, L., Forrest, D., Vennstrom, B., and Larsson, L. (2000). Effects of thyroid hormone receptor gene disruption on myosin isoform expression in mouse skeletal muscles. Am J Physiol Regul Integr Comp Physiol *278*, R1545-1554.

Zechner, C., Lai, L., Zechner, J.F., Geng, T., Yan, Z., Rumsey, J.W., Collia, D., Chen, Z., Wozniak, D.F., Leone, T.C.*, et al.* Total skeletal muscle PGC-1 deficiency uncouples mitochondrial derangements from fiber type determination and insulin sensitivity. Cell Metab *12*, 633-642.

Zhang, C.L., McKinsey, T.A., and Olson, E.N. (2002). Association of class II histone deacetylases with heterochromatin protein 1: potential role for histone methylation in control of muscle differentiation. Mol Cell Biol *22*, 7302-7312.

VITAE

Daniel Simon Quiat was born in Concord, CA on March 27th, 1984, the son of Allan and Jean Quiat and brother of Eric Quiat. After graduation from Cypress Springs High School in Houston, TX in May 2002, he enrolled at the University of Texas in Austin. While at UT-Austin, he performed research in the laboratory of Dr. David Parichy, studying the genetics of pigment pattern formation and neural crest cell migration in zebrafish. He graduated *Cum Laude* with a Bachelor of Science(B.S) in December 2005, and subsequently worked as a research assistant in the laboratory of Dr. Jeffery Gross studying ocular lens development in zebrafish. In June of 2006, he enrolled in the Medical Scientist Training Program at University of Texas Southwestern Medical Center. On October 23rd, 2011, Daniel married Elizabeth Rose Dreyfuss in Dallas, TX.

Permanent Address: 4104 N Hall #102
Dallas, TX 75219